Stress-induced community tolerance of stream biofilms grown at contrasting hydrodynamic conditions

Thesis submitted for graduation with the academic degree of

"Master of Science"

by

Bastian Herbert Polst

(01450358)

Supervised by

Prof. Dr. Thomas Hein (Supervisor)

Dr. Mechthild Schmitt-Jansen (Co-Supervisor)

Master programm: Applied Limnology (H 066 448)

Institute of Hydrobiology and Aquatic Ecosystem Management (IHG), University of Natural Resources and Life Sciences, Vienna

In cooperation with the Department for Bioanalytical Ecotoxicology, Helmholtz Centre for Environmental Research UFZ, Leipzig

Acknowledgments

First of all, I want to thank Dr. Mechthild Schmitt-Jansen for the opportunity to conduct the research for my master thesis under her supervision. Also, thanks to my Prof. Dr. Thomas Hein for co-supervision. Secondly, I want to thank Dr. Ute Risse-Buhl, Christine Anlanger and the Department of River Ecology at the UFZ Magdeburg for their help with the experiment and it's associated tasks.

I want to thank everyone who made my stay at the UFZ Leipzig enjoyable. Especially I am grateful to Stephan Lips, Dr. Floriane Larras, Christoph Rummel and Iris Christmann for the support in the laboratory and helpful discussions.

Last but not least, I thank my family and friends for constant support during my master study in Vienna and my master project in Leipzig. I'm deeply grateful to Patricia Geesink. You were my motivation to study hard and my biggest helper in time of need.

Affidavits

I hereby declare that I am the sole author of this work. No assistance other than that which is permitted has been used. Ideas and quotes taken directly or indirectly from other sources are identified as such. This written work hast not yet been submitted in any part.

Abstract

Biofilms in rivers are complex communities built of bacteria, fungi, algae and protozoa embedded in a matrix of extracellular polymeric substances (EPS). They are important hotspots for biogeochemical processes in aquatic systems. A variety of stressors can potentially affect the structure and function of biofilms. Their stress response, which depends on their exposure history, may influences their tolerance towards another stressor. Community composition and physical structure is influenced by hydrodynamics. Even though biomass and thickness of biofilms were reported to decrease with higher mean flow velocity and turbulence, the cell-to-EPS ratio increased. Therefore, differences in community tolerance towards herbicides are expected for biofilms grown under variable flow conditions. The interactive effects of hydrodynamic growth conditions and herbicide tolerance are lacking, especially due to the inadequate quantification of hydrodynamic conditions. Using an artificial flow-through channel and water from the River Selke (Elbe catchment, Germany), we created heterogeneous flow regimes and related biofilm community structure and function to different mean flow velocities and values of turbulent kinetic energy. Taking the biofilms grown under such controlled hydrodynamic conditions, herbicide tolerance towards prometryn was tested according to the PICT-approach. Focusing on the phototrophic part of the biofilm communities, we 1) investigated the biofilm community, the EPS matrix and the herbicide tolerance under different hydrological regimes and 2) assessed the role of EPS in stressor interactions. The relevance in EPS-content in combined stressor interactions was confirmed by using artificial EPS and an algal monoculture (*Nitzschia palea*).

Keywords: biofilm, multiple stressors, microbial communities, PICT, near streambed hydrodynamic conditions

Zusammenfassung

Biofilme in Flüssen bestehen aus einer komplexen Gemeinschaft von Bakterien, Pilzen, Algen und Protozoen, welche in einer Matrix aus extrazellulären polymerischen Substanzen (EPS) vorkommen. Unter anderem dienen sie als wichtige biogeochemische Hotspots in Gewässern. Ihr Verhalten bei Stress basiert auf eventuellen vorangegangen Expositionen und beeinflusst möglicherweise das Verhalten anderer Stressoren gegenüber. Während die Masse und Dicke der Biofilme mit steigender Fließgeschwindigkeit abnehmen, steigen andere Parameter, z.b. das Zell-zu-EPS Verhältnis an. Diese Veränderungen lassen Unterschiede im Verhalten, respektive der Toleranz, von Biofilme in unterschiedlichen hydrodynamischen Bedingungen gegenüber Herbiziden erwarten. Untersuchungen zu dem Zusammenspiel dieser Effekte fehlen jedoch, was hauptsächlich durch die unzureichende Erfassung hydrodynamischer Bedingungen zurückzuführen ist. Eine künstliche Fließrinne nutzend wurden mit Wasser der Selke (Zufluss zur Elbe) unterschiedliche hydrodynamische Bedingungen erzeugt. Verschiedene Parameter der Biofilme wurden mit den durchschnittlichen Fließgeschwindigkeiten und Werten der turbulenten kinetischen Energy (TKE) korreliert. Diese Biofilme wurden genutzt um die Toleranz gegenüber dem Herbizid Prometryn nach dem PICT-Schema zu testen. Auf den phototropischen Teil der Biofilmgemeinschaften fokussierend, wurde 1) getestet ob sich die Diatomen Gemeinschaft, die EPS-Matrix und die Biofilm-Toleranz unter verschiedenen hydrodynamischen Bedingungen unterscheidet. Weiterhin wurde 2) die Rolle der EPS-Matrix auf die Stressor Interaktion untersucht. Die Bedeutung der EPS-Matrix wurde in einem zweiten Experiment mit künstlichem EPS und einer Algenmonokultur (*Nitzschia palea*) bestätigt.

Keywords: Biofilm, multiple Stressoren, Mikrobielle Gemeinschaften, PICT, Flussbettnahe hydrodynamische Bedingungen

Content

List of Figures

List of Tables

List of Abbreviations

TKE: Turbulent Kinetic Energy

EPS: Extracellular polymeric substances

PAM: Pulse-amplitude modulated

SP: Saturation pulse

AL: Actinic light

Y(I): Yield I

Y(II): Yield II

EC50: Effective concentration at 50% of inhibition

DMSO: Dimethylsulfoxid

TN: Total Nitrogen

TP: Total Phosphorous

BP: Bound Phosphorous

SRP: Soluble reactive Phosphorous

1   Introduction

In streams and rivers, benthic biofilms play a crucial role in terms of primary production and biogeochemical processes *(Battin et al.,2003b)*. Often also referred to as periphyton, aquatic biofilms cover a wide range of different taxonomic kingdoms, e.g. fungi, bacteria, archaea, algae, protozoa and viruses, joined in a community (Larned,2010). In biofilms these organisms live attached to surfaces within the stream channel bed, where benthic biofilms form a unique microhabitat for aquatic microorganisms (Battin *et al.*,2016). Embedded in a matrix of extracellular polymeric substances (EPS), the biofilm organisms shape their own microecosystem (Flemming and Wingender,2010). Furthermore, biofilm are dynamic systems that can adapt to different environmental conditions regarding light, nutrients, pollution and hydrologic regimes (Villeneuve 2011).

Playing a major role for aquatic ecosystems, biofilms but also aquatic systems in general suffer from different stressors and the majority of European rivers have an ecological status of "moderate" or worse (EEA,2012). Approximately two third of European rivers are affected by two or more stressors at the same time (Schinegger *et al.*,2012). Water quality pressures (59% of European rivers) and alterations of hydrology due to channelization or impoundments (41% of European rivers) are widely distributed. Still, chemical and toxic stressors are underrepresented in current research (Nõges *et al.*,2016; Schafer *et al.*,2016).

The flow affects structural and functional parameters of biofilms, e.g. primary production, biodiversity and internal mass transport decreases with increasing flow velocity (Lau and Liu,1993; Biggs and Hickey,1994; Beyenal and Lewandowski,2002; Larned *et al.*,2004; Soininen,2004). The algal composition of biofilms adapts to the present flow velocity (Graba *et al.*,2013). At the same time, basal layers of biofilms can be limited by insufficient nutrient acquisition and through shear stress at the tops of biofilm (Hondzo and Wang,2002). The EPS matrix is affected by different flow velocities as well and gets thinner but denser with increasing flow velocity (Wang *et al.*,2014). A similar role for the biofilm composition, architecture and biomass has the near streambed turbulences as highlighted in only a few studies (Labiod *et al.*,2007; Risse-Buhl *et al.*,2017). While the mean flow velocity only measures the one-dimensional

(longitudinally) flow. The TKE measures all three dimensions (longitudinally, laterally, vertically) and is a better descriptor for the complex physical environment (Statzner *et al.*,1988).

The same way the flow velocity acts as a controlling environmental factor in shaping biofilms, water quality (nutrients and organic pollution) affects the biofilm community as well. In European rivers 960 organic chemicals were found by Busch *et al.* (2016) of which 42% are pesticides, 165 compounds are potentially hazardous to algae and at least 7% inhibit photosynthesis. Targeting the Hill-reaction and decreasing the electron transport of the photosystem II (Shimabukuro and Swanson,1969; Arnaud *et al.*,1994), these herbicides decrease species richness, algae biomass and primary production (DeLorenzo *et al.*,2001). During chronic exposure herbicides also apply a species selection pressure on the biofilm community. Sensitive species vanish and tolerant species dominate the community. As a consequence a pollution-induced community tolerance (PICT) occurs (Blanck *et al.*,1988).

The response of stream biofilms towards herbicides in terms of changing biodiversity and primary productivity can differ due to the present species pool with different sensitivities. Hence, we expect the herbicide tolerance to be related to the hydrodynamic regimes that shapes the biofilm composition (Guasch *et al.*,1997; Pesce *et al.*,2006; Villeneuve *et al.*,2011). This link was tested under the "biological insurance hypothesis" (Yachi and Loreau,1999) by Villeneuve *et al.* (2011). While they could not link the herbicide sensitivity of biofilm communities to different flow velocities, they found a higher sensitivity in a more heterogeneous and turbulent flow channel. Still, parameters like the near streambed turbulence or the EPS matrix were not observed in their study.

I want to fill this gap of knowledge about the possible link of hydrodynamic conditions in terms of near streambed flow velocity and turbulence and herbicide sensitivity of stream biofilms. We hypothesize that:

1) The herbicide sensitivity of stream biofilms increases with increasing near streambed flow velocity and turbulence., which the hydraulic stress leads to a decline in the EPS matrix. This leads to a higher sensitivity towards herbicides (Lau and Liu,1993; Biggs *et al.*,2005).

2) The diversity of the diatom community decreases with increasing flow velocity, due to the hydrologic selection pressure (Soininen,2004; Graba *et al.,*2013).

Therefore, we take in charge the near streambed turbulence, measured as the turbulent kinetic energy (TKE), and the composition and mass of the EPS matrix. Using an artificial flow channel and river water to grown biofilms in different hydrologic regimes we tested their herbicide sensitivity *in vitro*.

2   Material and Methods

2.1   Pulse-amplitude modulated fluorometry

To measure the photosynthetic activity and their decrease due to the application of herbicides, we used the Pulse-amplitude modulated (PAM) fluorometry to determine the yield of the chlorophyll fluorescence. Under the photochemical pathway, photons are absorbed by the two photosystems of the chloroplasts. The pigment antenna transfer an electron to the primary quinone acceptor Q_a and the residual electron transport chain of photosynthesis (G. H. Krause,1991). The energy of the residual absorbed photons, which cannot be transported by the photochemical electron transport chain, needs to be emitted to prevent damage of the photosystems by either emission of heat or, preferably, fluorescence. The chlorophyll fluorescence accounts for 1-2% of the absorbed light under normal conditions and is emitted at longer wavelengths as the absorbed light (Maxwell and Johnson,2000).

The yield of the chlorophyll fluorescence can be used as an observation parameter to measure the efficiency of photosynthesis, since it increases once the capacity of the electron transport chain reached its maximum. Excitation light of a defined wavelength needs to be applied towards the algae (Maxwell and Johnson,2000). This is done using pulse-amplitude modulated (PAM) fluorometry where a saturation light pulse (650nm, 8000 µmol Photons m^2 s^{-1}) is used to quench the photosystem and promote a chlorophyll fluorescence based on the efficiency and capacity of the photosystems (Schreiber,1998). The chlorophyll fluorescence is measured before and after the application of the saturation pulse.

Measurements can be done of two stages of adaption of the chloroplast, the dark-adapted stage (Yield I) and the light-adapted stage (Yield II). While the dark-adapted stage is used to measure the maximum yield of the photosystem under dark conditions, the light adapted stage measures the effective yield of the photosystem under luminous conditions. For the dark-adapted yield, the samples are kept in darkness for a few minutes prior to the measurement of F_0. The light adapted stage is measured after application of an actinic light.

Figure 1 shows the typical chlorophyll fluorescence over the duration of a PAM fluorescence measurement after Maxwell & Johnson (2000). Once the measuring light (MB) is applied, the base

fluorescence F_0 is measured. When a saturation pulse (SP) is applied, the fluorescence increases and gives the maximum possible chlorophyll fluorescence (F_m^0). After the measurement of the dark-adapted yield, an actinic light (AL) is applied to simulate luminous conditions. After a given time of adaption towards the new conditions, the light-adapted base fluorescence is measured F_t and another saturation pulse is applied. The chlorophyll fluorescence increases again and is measured (F_m').
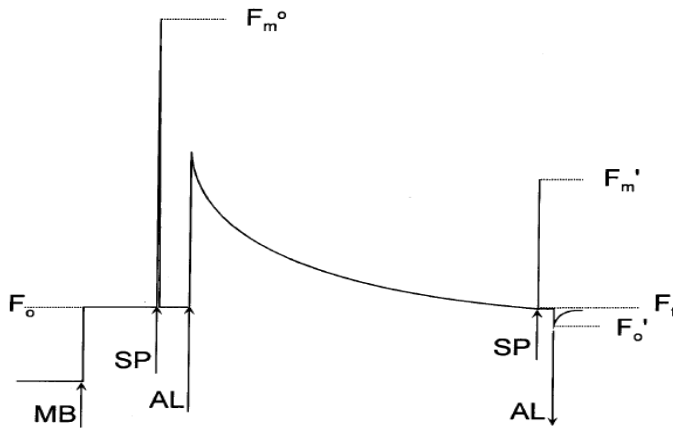
Figure 1: The sequence of a typical chlorophyll fluorescence trace. A measuring light (MB) is switched on and the zero-fluorescence level is measured (F_0). Application of a saturating flash of light (SP) allows measurement of the maximum fluorescence level F_m^0. A light to drive photosynthesis (AL) is then applied. After a period of time, another saturating light flash (SP) allows the maximum fluorescence in the light (F_M') to be measured. The level of fluorescence immediately before the saturating flash is termed F_t. Turing of the actinic light (AL), typically in the presence of far-red light, allows the zero level of fluorescence (F_0') in the light to be measured. (after Maxwell & Johnson (2000))

The quantum yields of photosynthetic energy conversion in PSII of the two adaption-stages are calculated with the following equations according to Genty *et al.* (1989):

$$Y(I) = \frac{(F_m - F_0)}{F_m}$$ for the dark-adapted stage (maximum quantum yield)

$$Y(II) = \frac{(F_{m'} - F_{0'})}{F_{m'}}$$ for the light-adapted stage (effective quantum yield)

2.2 Inhibition of photosynthesis caused by herbicides

The most applied mode of action of herbicides refers to the inhibition of the photosystem II and the electron transport. As a final consequence, it stops the essential ATP-synthase. Already in 1991 the mechanism was discovered by Fuerst & Norman (1991), as the "PSII-inhibitors bind to the D1 reaction center protein and inhibit electron transport by acting as nonreducible analogs of plastoquinone". The plastoquinones are transporters of electrons within the electron transport chain and need to bind at the D1 protein to fulfill their function. As the place is irreversibly occupied by the herbicide, absorbed energy can no longer be transported along the ETR and is emitted by fluorescence. While the chlorophyll fluorescence increases, the calculated yield decreases.

2.3 Experiment 1: Comparison of attached and suspended biofilms

Suspended biofilms have the advantage of easier handling and faster processing. To test whether the use of suspended biofilms leads to different results, the following experiment was conducted.

Biofilms were grown in an aquarium on glass slides and glass disks (1.5cm²). Twenty-four disks and four slides were sampled after four weeks. Their backsides, which were in touch with the rack, were scratched off and discarded to ensure equal conditions. Photosynthesis of attached biofilms on slides was measured using the Imaging-PAM fluorimeter (IMAGING-PAM, M-Series, Walz, Germany, Measuring & Actinic light conditions: Intensity 4, Gain 4, Damping 2). Afterwards, the biofilms which were grown on the front side, were scratched off and pooled in a 16 mL suspension of filtered (0.2µm, Polyvinylidendifluorid, Macherey-Nagel, Germany) Parthe (Weiße Elster catchment) water. A volume of 0.5mL of this biofilm suspension was added to each well of a first 24-well plate. The twenty-four disks with the attached biofilm were placed in a second 24-well plate. Each well was filled up to a volume of 2mL with filtered (0.2 µm) Parthe water. Both, the well plate with the disks and the one with the suspensions, were measured with the Imaging-PAM (I-PAM) under the same conditions as before. Afterwards, a logarithmic dilution row consisting of six concentration steps of the herbicide Prometryn, dissolved in Dimethylsulfoxid (DMSO, SigmaAldrich), was added to both plates in triplicates each (83.9 µmol L^{-1} – 0.00084 µmol L^{-1}). After an exposure of one hour under light and shaking at 100 rpm (IKA Labortechnik, KS250 basic), both plates were measured again with the Imaging-PAM to determine the yield of the chlorophyll fluorescence through Prometryn. The plates then again were placed under light and slightly shaking conditions for another twenty-three hours. After overall twenty-four hours of herbicide exposure, the yield of the chlorophyll fluorescence was determined with the Imaging-PAM. The inhibition of the yield of the chlorophyll fluorescence was calculated based on the yield values of the DMSO-control of each plate at the specific time point. Dose-response curves were plotted based on the four-parametric hill-equation $y = y_0 + \frac{ax^b}{c^b + x^b}$ (y_0= the minimum value that can be obtained (0.0001), a = the maximum value that can be obtained (100), c = the point halfway between a and d (i.e. the EC50), b = Hill's slope at point c) with 1000 iterations per curve.

To determine changes in the algae classes, the slides were measured with the Phyto-PAM fluorimeter (Sensor: PHYTO-EDF, Walz, Germany) before the biofilm was scratched off. After the scratching-off, the biofilm suspension was measured with the Phyto-PAM.

After the twenty-four hours of herbicide exposure and the following Imaging-PAM measurement, the negative control samples were removed from the plates for further pigment extraction with acetone. Therefore, the suspended control samples were loaded onto a 0.2 µm filter, which underwent the same treatment as the disks with the attached biofilm. The algae-associated pigments Chlorophyll a, Chlorophyll b, Fucoxanthin, beta-Carotene, Alloxanthin, Zeaxanthin and Lutein were measured via High-Pressure Liquid Chromatography (HP-LC) (column: KNAUER Superspher-100 RP18, Berlin, Germany) based on the protocol by Schubert (2015).

2.4   Experiment 2: The flume experiment

Biofilms in different hydrodynamic conditions were developed using an artificial flow channel fed with water constantly extracted from the neighbouring Selke river. The hydrodynamic conditions were classified through measurements of the near streambed flow velocity and turbulence. After four weeks, the biofilms were sampled and an *in-vitro* herbicide assay was conducted. Furthermore, the EPS content and composition was measured, as well as the species composition of the diatom community.

2.4.1   Study site

Located in the eastern German region of Sachsen-Anhalt, the River Selke flows through the low mountain range Harz and conservation area "Selketal" as well as the Flora-Fauna-Habitat (FFH) region "Bode und Selke im Harzvorland (FFH0172)" (Natura2000-LSA,2017). The catchment is dominated by deciduous forests on the hills and grassland on the valley bottom (Figure 2). Through the low anthropogenic influences, the whole catchment is in a near-natural state. The Selke itself provides habitats for a diverse fauna, e.g. *Cinclus cinclus*, *Tritusus alpestris* and *Cottus gobio* ((LVWA-SachsenAnhalt,2017).

Figure 2: The Selke valley upstream of the flume channel (red mark) is characterized by deciduous forests, grassland and a low anthropogenic influence. The blue arrow is indication the flow direction. (after Risse-Buhl (personal communication) and Google Maps© (28.06.2017).

Near the end of the Selke-valley, approximately two kilometers south of Meisdorf, a so called "Mobile Aquatic Mesocosm" (MOBICOS) container, operated by the Helmholtz-Center for Environmental Research UFZ, is located next to the stream. The MOBICOS container functions as experimental laboratory facility, containing the artificial flow channels.

2.4.2 The flow channel

In the first part of the experiment biofilms under different hydrodynamic conditions were cultivated, targeting the first two research questions.

The flow channel (length: 5.2 m, width: 0.5 m), was designed and constructed at the Helmholtz-Centre for Environmental Research GmbH (Figure 3a). The inflow and outflow sections are made of stainless steel, while the experimental section (length: 3.0 m, width: 0.3 m) is made of float glass elements. Water of the Selke was pumped through a filter system (5 mm mesh size) to avoid debris and macro-organisms in the flow channel, passing a set of three perforated plates do dampen the inflow driven turbulence into the flow channel. The water level is controlled by a weir placed at the end of the outflow section. Discharge was monitored by a clamp-on ultrasonic flowmeter (MB 100H, Messbar, Aschheim-Dornach, Germany) installed at a tube section right before entering the flume and averaged 8.5 L s^{-1}. Biofilms were grown on large unglazed ceramic tiles (anthracite). To achieve diversity in the hydrodynamic regimes, a total of three jet-like flows were realized by trapezoidal shaped PVC nozzles located at both sides of the channel narrowing the cross-section of the flume to half of its area (Figure 3b). In the jet, the flow velocity increases and turbulent currents occurred, especially at the end of the narrowing. Four parallel LED-light (Solar Stringer SunStrip daylight, Econlux, Cologne, Germany) supplied biofilms with photosynthetic active radiation of 36.1 ±5.8 µmol m^{-2} s^{-1} (mean ±SD) for 10 hours a day.

The flume was operated for 34 days, from the 22nd March (16 o'clock) till the 25th April 2017 (22 o'clock). Over the whole duration, the water temperature and the oxygen concentration (Hobo U26, Onset Computer Corporation, Bourne, USA) were measured at the end of the flow channel every 15 minutes. Water-chemical parameters were measured on day 10, 13, 21, 25, 29 and 35. Total nitrogen and phosphorus and bound phosphorous were determined according to the DIN EN ISO 11905-1-H36 (1998) and 38405-11 (1983) for total nitrogen (TN), total and bound

phosphorous (TP, BP). Dissolved organic carbon (DOC), nitrate (NO3-N). Nitrite (NO2-N), ammonium (NH4-N) and soluble reactive phosphorous (SRP) were determined according to DIN EC ISO 13395-D28 (1996), 11732-E32 (2005) and 15681_Part_2-D46 (2005). Water chemical measurements were performed by U. Risse-Buhl and colleagues at the UFZ Magdeburg.

For the further experiment only the first section of the flow channel, ranging from the first two obstacles till the second, was used.

Figure 3: a) on the left, the flow channel with the artificial substrate (black tiles) is shown. b) On the right, one of the current obstacles, which will be placed on both sites at three transects, is shown.

2.4.3   Measurement of the flow velocity and turbulent kinetic energy

Three-dimensional current velocity measurements were conducted with a multi-static acoustic Doppler velocity ADV profiler (Vectrino II, Nortek AS, Norway) at 64 Hz for 5 minutes 2.3 cm above the flume bed. The ADV was mounted on a custom made instrumental carriage system allowing for positioning the measurement equipment at different points along the flume. Velocity timeseries were processed and turbulent kinetic energy TKE was expressed according to Risse-Buhl et al. (2017). Briefly, TKE is used as a measure for turbulence intensity which is calculated as

velocity fluctuations around a time-averaged mean. Furthermore, flow velocity U was calculated as $\langle U \rangle = \langle (u^2 + v^2 + w^2)^{0.5} \rangle$ where u, v and w denote the longitudinal, transversal and vertical component of the velocity vector respectively and angle brackets denote the time average.

2.4.4 Biofilm sampling procedure and sample partitioning

On the same positions as hydrodynamic measurements were performed (table 1), biofilm samples were taken using a self-build sampler (adapted from Eßer (2006), designed by Helge Norf and constructed by Peter Portius and his team from the UFZ Leipzig). The sampler was based on a toothbrush head within a sample chamber. When the sampler was placed on the tile surface, respectively the biofilm patch, the area around the sample was sealed and the toothbrush was placed on the sample. Under a constant flow of sterile filtered (0.2 µm, Sartorius, Göttingen, Germany) river water realized by a peristaltic pump the head of the toothbrush was pushed on the biofilm, rotated three times and pushed up and down three times. This procedure was repeated three times to ensure that the whole biofilm was detached at an area of 5.7 cm² and transported with the flow into the sampling tubes. Approximately 20 mL of suspended biofilm material was taken per patch. Samples were stored at 8°C until further use, which was within the next 12 hours. In total, six biofilm samples were harvested along a flow-velocity gradient (figure 4 and figure 5).

Table 1: Coordinates of the six samples within the flow channel. Since two neighbored patches were pooled for one sample, there are two X-coordinates for each sample, but only one Y coordinate. The coordinates represent the center of the circular sample patch.

Sample	X-Coordinate	Y-Coordinate
B1 🔴	33.5 & 38.5	0
B2 🟣	78.5 & 83.5	-10
B3 🔵	78.5 & 83.5	-5
B4 🟢	78.5 & 83.5	0
B5 🟠	78.5 & 83.5	5
B6 🔴	78.5 & 83.5	10
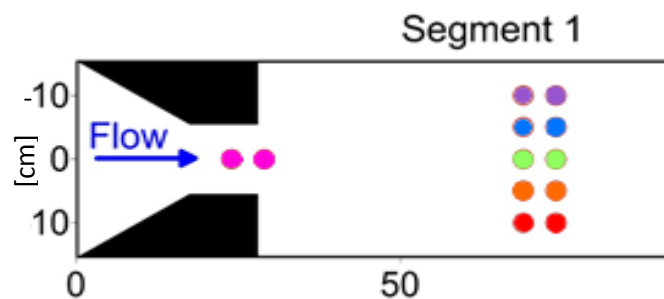
Figure 4: The samples within the first segment of the flow channel are shown true to scale. Samples are indicated by the colors shown in table 1 (on the left side). Part of the figure kindly provided by Christine Anlanger.
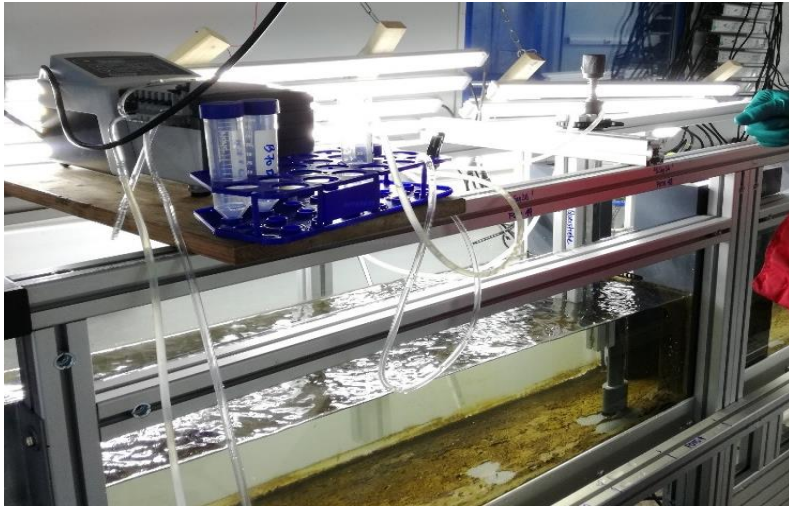
Figure 5: Sampling of the biofilms in the flow channel was performed under active flow of water. The sampler (bottom right) seals the area around the biofilm sample. A toothbrush is used to detach the biofilm. The biofilm suspension was then pumped into 50 mL falcon tubes.

To decrease the volume of the biofilm suspension, the biofilm particles were allowed to settle down for 8 hours over night at 4°C and were subsequently centrifuged at 2000 g for 5 minutes (2k15 Centrifuge, Sigma, Osterode, Germany). Afterwards, the supernatant was removed until a volume of 5 mL per sample was left. In the end, the biofilm samples were suspended in 5 mL of sterile filtered Selke water. The complete procedure with the biofilm samples is shown in figure 6.

Then the biofilm samples were divided into two subsamples, 3 mL were used for the PICT-herbicide assay (chapter 2.4.5) and 2 mL were used for the extraction of EPS (chapter 2.4.6).

The biofilm samples used for the herbicide assay were used for the diatom analysis afterwards (chapter 2.4.7). At the same time, the EPS matrix, consisting of the bound and the soluble fraction, was extracted resulting in 4 mL of both fractions per sample. Both fractions were analyzed for Carbohydrates, Proteins, Humic acids and Uronic acids. These four compartments of both fractions together were considered to sum up for the total EPS content of each sample (McClellan,2006).
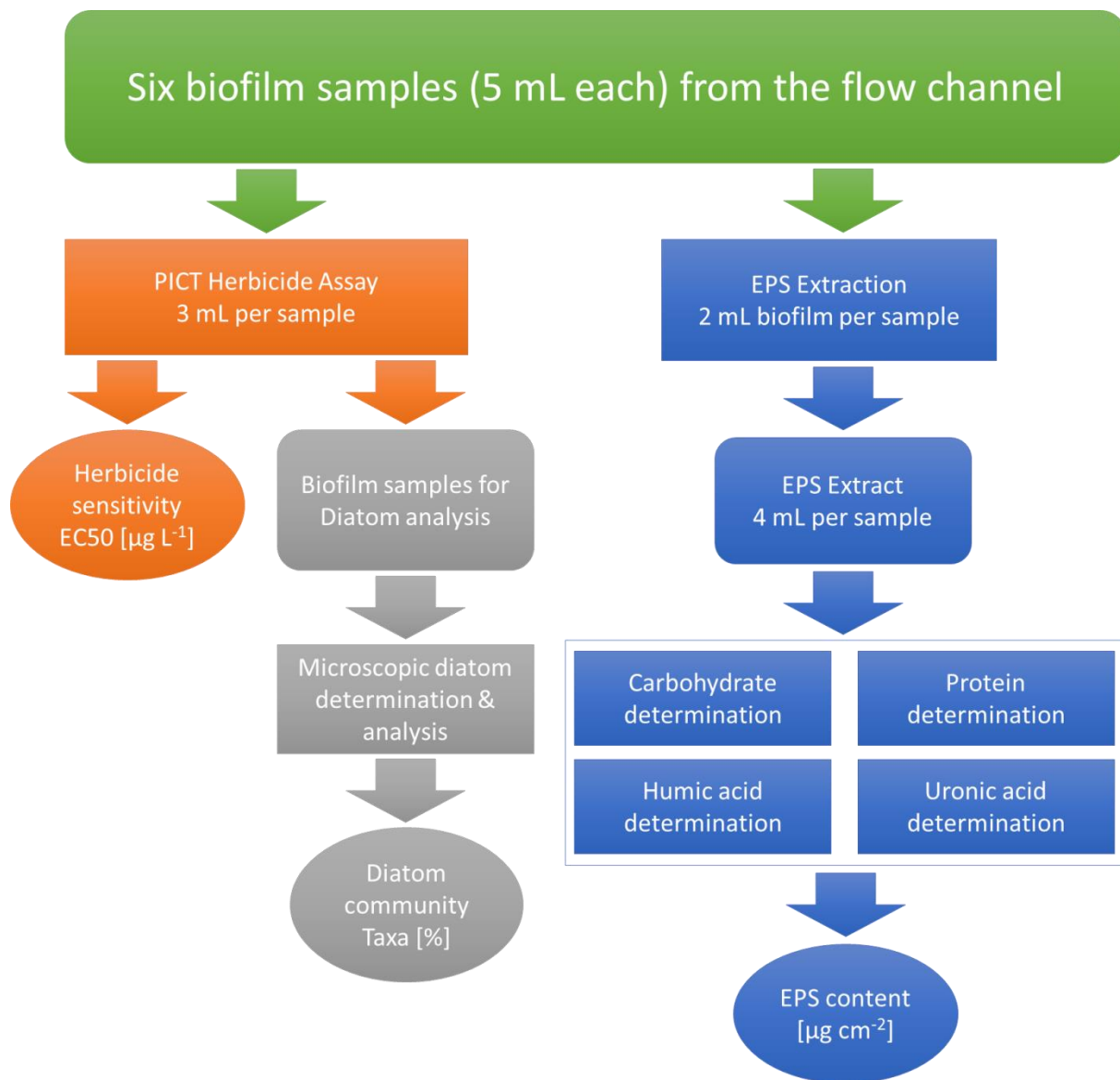
Figure 6: Work flow of the processing of the biofilm samples. After suspending the biofilm samples in a final volume of 5 mL per sample, 3 mL were used for the PICT-Herbicide assay and 2 mL were used for the EPS Extraction. A subsample of the biofilm sample was used for the analysis of the diatom community. In the end of all work, the EC50 values, the diatom community and the composition and mass of the EPS was derived.

2.4.5 Stress induced community tolerance -herbicide assay

To test the tolerance of the biofilms towards the herbicides the samples were exposed to seven different concentrations of the PSII-inhibiting herbicide Prometryn. The herbicide Prometryn was selected due to the high concentrations recently found by Rotter *et al.* (2015). Using 96-well plates, aliquots of 150 µL of the biofilm samples were taken under constant stirring to ensure

homogeneity. For each dilution step of the herbicide, three biofilm subsamples were. A Dimethylsulfoxid (DMSO, SigmaAldrich) control was also used in triplicates final DMSO concentration: 0.005 %).

To measure the chlorophyll fluorescence with the Imaging-PAM (Walz, Effeltrich, Germany) the herbicide Prometryn was dissolved in DMSO. Due the possible toxic effect of DMSO on the biofilms, the DMSO-herbicide solution needed to be diluted with bi-distilled water to a concentration of 0.1% DMSO. Biofilm samples were inoculated with the dissolved Prometryn at six different concentrations in triplicates within a 10-fold dilution row ranging from 0.00084 µmol L^{-1} to 83.8 µmol L^{-1}. The fluorescence was measured at dark- and light-adapted conditions one hour and twenty-four hours after the initial herbicide exposure. Then, the 96-well plates with the biofilm-herbicide suspension were placed under light and intense shaking at 350 rpm (IKA Labortechnik, KS250basic). After one hour, the fluorescence was measured with the Imaging-PAM fluorimeter at both, the light- and dark-adapted, conditions. Afterwards, the samples were again placed under light with intense shaking for another twenty-three hours. Twenty-four hours after the initial herbicide exposure, the measuring procedure using the Imaging-PAM-fluorometer was repeated for a second time. Results were analyzed with the software SigmaPlot 13.0 (Systat Software GmbH, Erkrath, Germany). Dose-response curves were plotted based on the four-parametric hill-equation as shown in chapter 2.3.

a) b)
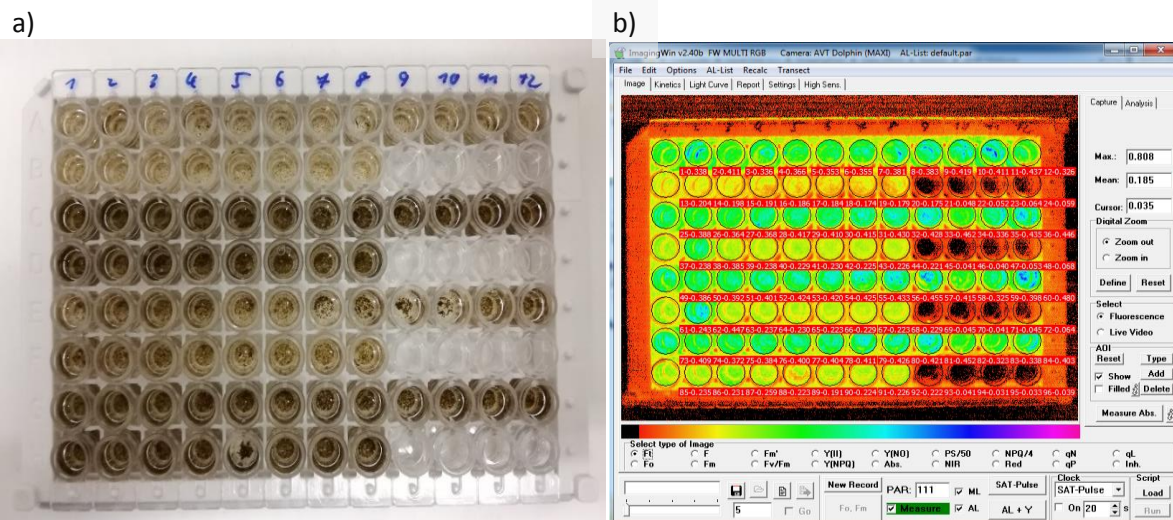
Figure 7: The 96-well plate with the biofilm samples used for the SICT-herbicide assay a) before and b) during the measurement with the Imaging-PAM.

2.4.6 EPS-extraction and determination of the biofilm samples

The EPS extraction was done after the method proposed by Barranguet *et al.* (2004). For the extraction of the biofilm-EPS matrix 2 mL per sample of the biofilm suspension were used. Two fractions were extracted, the soluble and the bound EPS-fraction. To extract the soluble fraction, the sample was vortexed and centrifuged for 5 min at 3500 rpm (2K15 Centrifuge, Sigma, Osterode, Germany). The supernatant was collected and the same procedure was conducted after the residual biofilm pellet was resuspended in 2 mL of bi-distilled water. Afterwards both 2 mL extractions of the soluble EPS fraction were pooled. From the residual biofilm pellet the bound EPS fraction was extracted. The pellet was suspended in 2 mL of 0.1 M H_2SO_4 and incubated at 95°C for 30 min (peQlab Thriller, Bremen, Germany). After centrifuging at 3500 rpm for 5 min the supernatant was collected. This was done two times and afterwards the two extracts of the bound EPS fraction of the same biofilm sample were pooled. All samples were stored at -80°C until further usage.

The EPS extracts were analyzed for their concentration of Carbohydrates, Proteins, Humic acids and Uronic acids. Chemicals used and solutions compounded are shown in annex I and II.

Carbohydrates

The carbohydrates of both EPS fractions were quantified according to DuBois *et al.* (1956). A serial dilution (25, 50, 100, 150, 200 mg L^{-1}) of D-Glucose-monohydrate ($C_6H_{12}O_6*H_2O$) was freshly prepared, based on a 1 g L^{-1} D-Glucose-monohydrate/bi-distilled water stock solution. Samples were done in triplicates. To each 200μL biofilm sample, D-Glucose-monohydrate dilution and negative control, consisting of bi-distilled water only, 200 μL 5% Phenol and 1 mL 95% H_2SO_4 were added. After incubating at 30°C for 35 min at 300 rpm the biofilm samples, the standard and the blank were measured at 488 nm against bi-distilled water in the UV/VIS photometer (UVIKON 923 Double Beam UV/VIS Spectrophotometer, Bio-Tek Kontron Instruments, Neufahrn, Germany). Concentrations of carbohydrates in the samples were calculated based on the absorbance of the standards.

Proteins and humic acids

The Protein and humic acid protocol is based on Lowry *et al.* (1951). A serial dilution (20, 40, 80, 120, 160 mg L^{-1}) was prepared based on a 200 mg L^{-1} bovine serum albumin (BSA) stock solution with bi-distilled water. Samples were done in triplicates. To each 250 µL sample, BSA standard and blank 250µL of 2% SDS and 700µL solution 4 (see annex I & II) were added. After incubation at 30°C over 15 min 100µ of solution 6 was added. To ensure a complete reaction, samples were incubated at 30°C over 45 min at 300 rpm (peQlab Thriller, Bremen, Germany). Afterwards, the samples were measured at 750 nm against bi-distilled water in the UVIKON photometer.

For the humic acid assay, a serial dilution (20, 40, 80, 120, 160mg L^{-1}) was prepared based on a 100 mg L^{-1} humic acid stock solution. To each 250 µL sample/standard/blank 250µL 2% SDS and 700 µL solution 5 (see annex I & II) were added. After incubation at 30°C over 15 min 100 µL solution 6 (see annex I & II) was added to each sample. After the final incubation at 30°C over 45 min the samples were measured at 750 nm in the UVIKON photometer. Since the measurement of Proteins and Humic acids interferences with each other, the values needed to be corrected based on Frolund *et al.* (1995).

Uronic acid

A protocol by Blumenkrantz & Asboe-Hansen (1973) and its modification by Kintner & Van Buren (1982) was used to assess the Uronic acid content in the EPS samples. A serial dilution (5, 10, 20, 30, 50, 80 mg L^{-1}) was prepared based on a 100 mg L^{-1} D-Glucuronic acid ($C_6H_{10}O_7$) stock-solution with bi-distilled water. 200 µL of each sample, standard-dilution series and blank were cooled on an ice bath beforehand. Then, 1.2 mL of solution 6 (see annex I & II) was added. Samples were incubated at 99°C for 5 min at 300 rpm (peQlab Thriller, Bremen, Germany). Afterwards, they were cooled again in the ice bath and 20 µL solution 7 was added (see annex I & II). After 20 min the samples were measured against bi-distilled water at 520 nm in the UVIKON photometer.

Based on the different dilutions of the standard, which were measured along with the samples, a linear trend curve was fitted. Based on the formula of the curve and the measured values of the samples, the final concentration per sample was calculated. The mean values of the soluble and bound EPS of each fraction were added to get the total content of each fraction.

2.4.7 Taxonomic analysis of the Diatom community

To prepare the diatoms of the biofilm samples for the mounting on glass slides, a protocol based on Bertzen & Müller (2002) and UCL_Department_of_Geography (2017) was used. Samples were stored in a 10%-Formalin (CH_2O, SigmaAldrich) solution before further usage. Of the in-Formalin-stored biofilm samples, 0.5 mL were used for the diatom reprocessing. A few drops of concentrated hydrochloric acid (35% v/v) were added and samples were heated to 80°C until full evaporation of the solution to dissolve residual chalk and to split the two parts of the diatom frustules. Afterwards the precipitations were cleaned with bi-distilled water twice and 0.5 mL hydrogen-peroxide (H_2O_2) were added. Samples then were heated to 80°C to remove organic material. The H_2O_2 than was decanted and the samples were washed with bi-distilled water until a neutral pH was achieved and finally stored in 0.5 mL bi-distilled water.

To mount the diatoms on glass slides the mountant Naphrax® (Biologie-Bedarf Thorns, Germany) was used. Therefore, 50 µL of the processed samples were given on a glass slide and heated at 50°C till evaporation of the water was complete. Afterwards, a drop of Naphrax was applied to the precipitated diatoms on the glass slide and heated at 60°C for 1 hour to evaporate the Toluol of the Naphrax. Of each sample, three slides were produced so the community could be assessed in triplicates.

To analyze the mounted diatoms a Leica DMI4000B microscope (Leica, Wetzlar, Germany) connected with a Leica PFC250 camera (Leica, Wetzlar, Germany) and the software Leica Application Suite Version 3.8.0 were used. Under a 630x zoom and bright field microscopy the diatoms were determined using recent literature and databases. Thereto, Hofmann *et al.* (2013), WesternDiatoms (2017), Guiry & Guiry (2017), Kelly *et al.* (2005) were used. Three slides per sample were produced. On each slide 400 frustules were determined, if possible on species level.

The diatom communities were assessed by using the software OMNIDIA (version 7.0). The calculation of several biological indices, the Shannon-Wiener-Index (H_s) and the evenness (E_h) were done by the software automatically after the following equations.

Shannon-Wiender-Index (H_s):

$$H_s = -\sum_{i=1}^{S} p_i \times \log p_i \qquad \text{with } p_i = \frac{n_i}{N}$$

S = Number of present species, N = total number of individuals, n_i = number of individuals per species, p_i = relative abundance of the i-species

Evenness (E_h):

$$E_H = \frac{H_S}{H_{max}}$$

H_{max}= maximal possible Shannon-Index, which would occur if each species would have the same relative abundance

2.5   Experiment 3: Influence of artificial EPS on the herbicide toxicity

To test the hypothesis resulting from the flow channel experiment, whether the EPS matrix absorbs and inhibits the herbicide, biofilms of the diatom species *Nitzschia palea* (Strainnumber 1052-3A, SAG Göttingen, Germany) were exposed to different concentrations of each EPS-fraction's standard substance of the EPS-assay (see 2.4.6) within a 24-well herbicide assay. *Nitzschia palea* (initial concentration: 1×10^6 cells mL^{-1} determined with Casy CellCounter, Bremen, Germany) biofilms were grown within the diatom-media (see annex IV) and under permanent illumination on 2 cm² glass disks in a 24-well plate for 2 days. After this period, the old media was exchanged with a new charge, which was enriched by different concentrations of dissolved artificial EPS, namely the standard substances used to determine the EPS content in chapter 2.4.6. D-glucosemonohydrate (Carbohydrate fraction), Humic acid (Humic acid fraction), BSA (Protein fraction) and Glucuronic acid (Uronic acid fraction) were added in the concentrations of 0, 25, 50 and 100 mg L^{-1}, representing the range of the single fractions found in the biofilm samples from the hydrodynamic channels (see chapter 2.4.6). Additionally, a mix of the four fractions, based on the mean ratio of the flume channel samples (Carbohydrates: 38.86%, Proteins: 30.86%, Humic acids: 25.90%, Uronic acids: 4.38%), was added in the concentration of 0, 50, 100, 200 and 400 mg L^{-1}. After the exchange with the enriched media, six different concentrations of Prometryn (20-fold, dissolved in DMSO) were added to the wells with the *N. palea* biofilms. The final concentrations in the wells ranged from 83.2 µmol L^{-1} to 0.00026 µmol L^{-1} Prometryn with a share of 0.1% DMSO. A DMSO-control and a negative (prometryn and DMSO-free) control were also used. For each concentration triplicates were used. After one hour and twenty-four hours after the initial herbicide exposure, the yield of the chlorophyll fluorescence was measured with the Imaging-PAM fluorimeter (Walz, Effeltrich, Germany) (see 2.4.5).

3   Results

3.1   Experiment 1: Comparison of structure and function of attached versus suspended biofilms

3.1.1   Photosynthetic Yield of attached versus suspended biofilms

The mean Yield I and Yield II of the attached and still intact biofilms on the slides are significant higher (Students t-test: $p < 0.05$) than the Yields of the suspended biofilms (Figure 8). Furthermore, the intra-suspension variation is significant lower than the one of the disks with attached biofilm (Levene-test: $p < 0.05$).
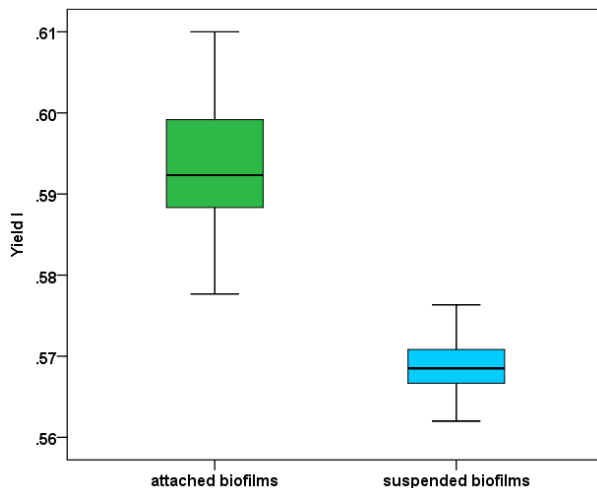
Figure 8: Maximal quantum yield (PAR 0) for comparison of a) the attached (n=32) and suspended biofilms of the four glass slides (n=24) and b) the attached biofilm on the disks and the biofilm suspension from the slides (n=24).

3.1.2   Relative abundance of algae classes & pigment analysis of attached versus suspended biofilms

The measurements of the algae classes, in particular for green algae and diatoms, show a high variation in suspension in comparison to attached biofilms (Figure 9). Cyanobacteria show a small deviation. When comparing the contribution of the algae classes of the attached and suspended biofilms, cyanobacteria show a significant difference ($p < 0.05$) and green algae and diatoms do not differ significantly.
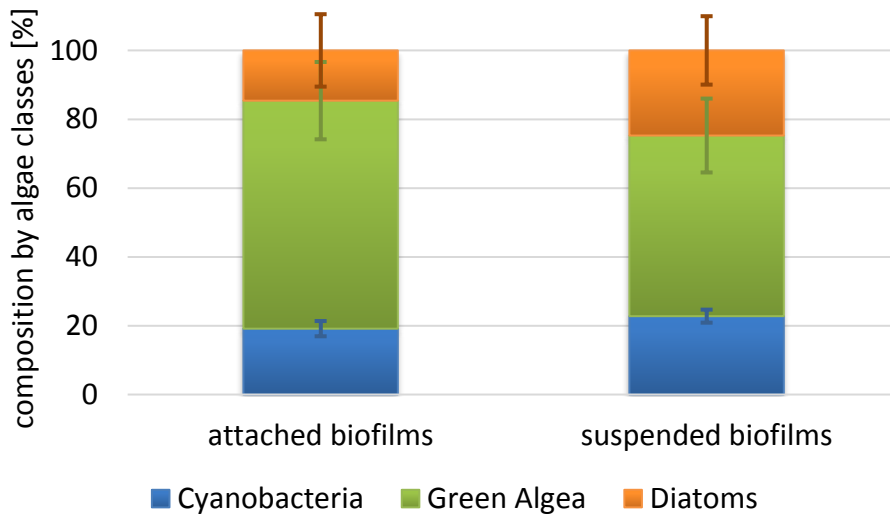
Figure 9: The mean percental composition of algae classes measured with the Phyto-PAM fluorimeter is shown before and after scratching off and suspending the biofilms afterwards. The standard deviations for the measurements before and after this process are displayed in the legend (n=13).

The HPLC analysis of the algae-associated pigments, showed significant differences for chlorophyll a measurements (Figure 10). The other pigments (Fucoxanthin, Beta-Carotene, Chlorophyll b, Alloxanthin, Zeaxanthin, Lutein) show a higher variation for the attached biofilms and no significant difference for the comparison between attached and suspended biofilms.
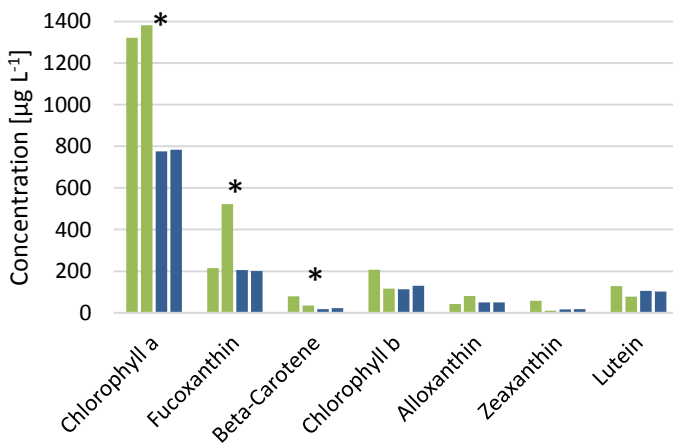
Figure 10: The algae-associated pigments for the attached biofilms (green) and the suspended biofilms (blue). Significant differences between the two treatments are indicated by the * and found for Chlorophyll a, Fucoxanthin and Beta-Carotene.

3.1.3   Sensitivity towards Prometryn of suspended versus attached biofilms

The inhibition of Yield I of the maximal chlorophyll fluorescence is lower for the attached biofilm in comparison with the biofilm suspension after an exposure of one hour (Figure 11). The EC50-value of the attached biofilms is approximately four times higher than the one of the suspended biofilms (7.38±1.80 & 1.93±0.46 µmol L^{-1}). After twenty-four hours, the EC50 values decrease approx. about factor 3 for the attached and factor 2 for the suspended biofilms. Although the difference of the EC50-value between the two treatments gets smaller, the EC50-values for both time points are significantly different (2.18±0.89 & 0.74±0.28 µmol L^{-1}).
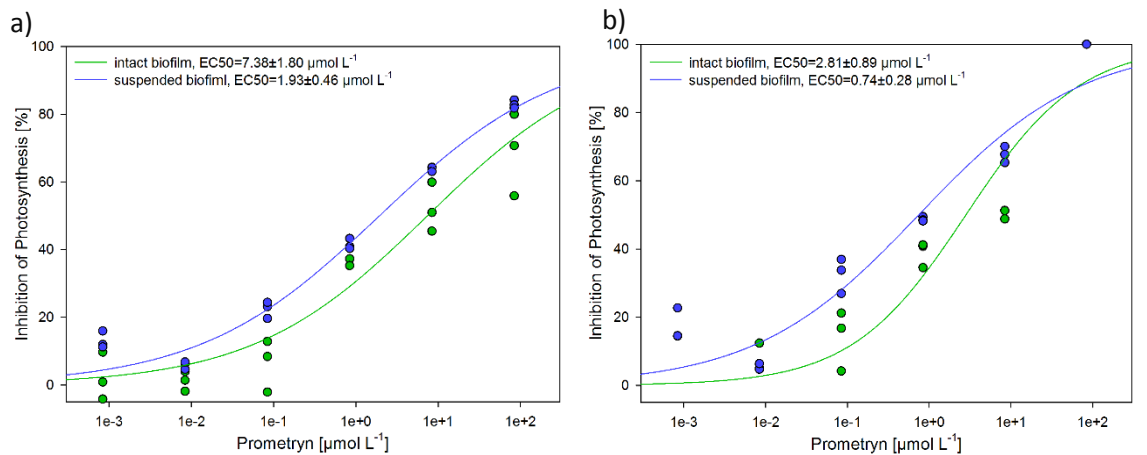
Figure 11: Concentration-effect curves for dark-adapted conditions after a) one hour and b) twenty-four hours of exposure. The curves are based on the Hill-equation (4 parameters, see 2.4.5).

The concentration-effect curves of Yield II show a high variation of inhibition for the attached biofilms (Figure 12). After one hour of herbicide exposure, the EC50-value of the attached biofilms (0.05±0.02 µmol L^{-1}) is two times lower than the value of the suspended biofilms (0.10±0.020 µmol L^{-1}). After twenty-four hours, the EC50-values overlap in their range defined by the standard-error (table 2; attached biofilms: 0.01±1.93 µmol L^{-1}, suspended biofilms: 0.02±0.01 µmol L^{-1}).
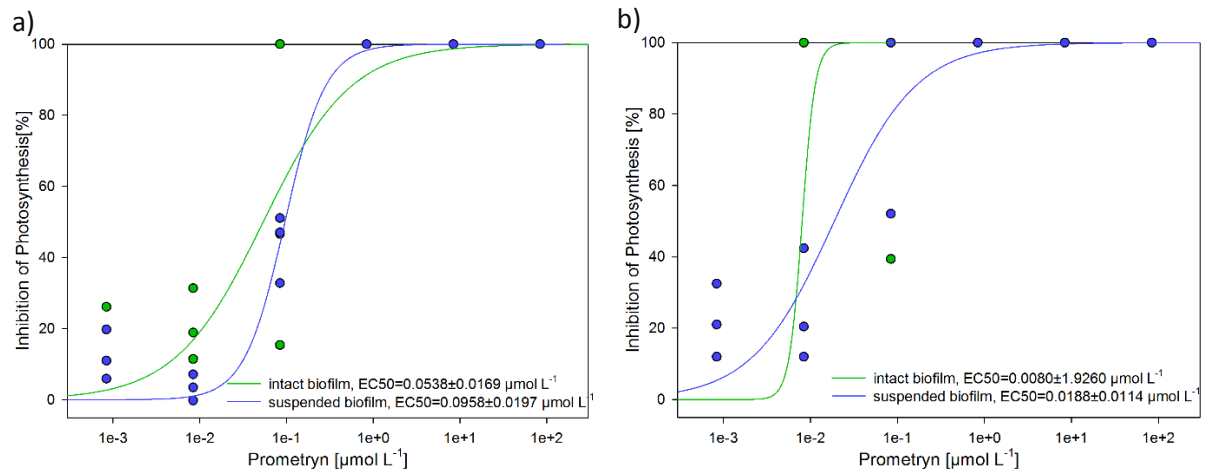
Figure 12: The concentration-effect curves (Hill-model with four parameters) for the light-adapted conditions after a) one hour and b) twenty-four hours.

Table 2: The parameters EC50±standard error (se), slope±se and R²of the dose-response curves of this experiment are shown.

Yield & Duration	Sample	EC50±SE [µmol L^{-1}]	Slope±SE [% µmol^{-1} L^{-1}]	R²
Yield I 1h	attached	7.38±1.80	0.41±0.04	0.9132±
	suspended	1.93±0.46	0.40±0.04	0.9766±
Yield I 24h	attached	2.81±0.89	0.62±0.11	0.8966±
	suspended	0.74±0.28	0.43±0.07	0.9284±
Yield II 1h	attached	0.05±0.02	0.86±0.21	0.8254±
	suspended	0.10±0.02	1.87±1.73	0.9755±
Yield II 24h	attached	0.01±1.93	5.79±31402.03	0.5887±
	suspended	0.02±0.01	0.92±0.44	0.8628±

3.2 Experiment 2: Hydrodynamic induced herbicide sensitivity of stream biofilms

3.2.1 Physico-chemical parameters in the flow channel water

The abiotic parameters shown in figure 13 and table 3 for the temperature show overall high
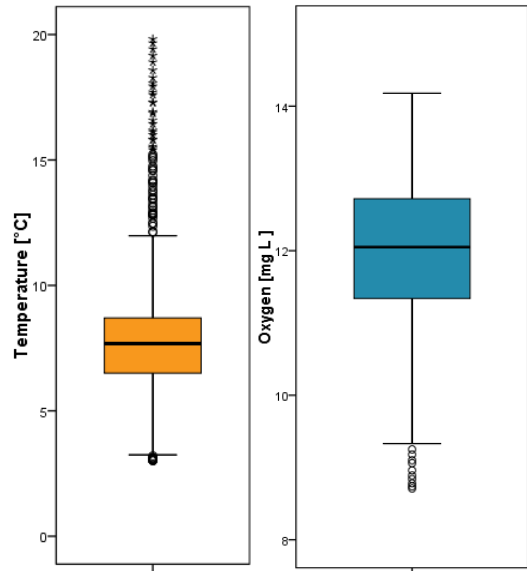
differences between the maximum and the minimum water temperature (min: 3.0°C, max: 19.8°C, also see annex III). The temperature averages at 7.72±1.91°C. The oxygen concentration ranges from approximately 9 mg L^{-1} to 14 mg L^{-1} and averages at 12.06±0.91 mg L^{-1}. Multiple measurements of the NH_4 and NO_2 are below the detection level. In general, the nutrient concentrations are on a low level.

Figure 13: The boxplots show the results of the continuous a) temperature and b) oxygen measurement in the flow channel. The circles represent outliers and the stars extreme values.

Table 3: Mean values and their standard deviation (SD) of the continuous temperature and oxygen measurements (n=3531) and the selective measurements (n=6) of NO_3, NH_4, NO_2, total nitrogen (TN), soluble reactive phosphor (SRP), total phosphor (TP), dissolved organic carbon (DOC), total organic carbon (TOC), total inorganic carbon (TIC), conductivity and the pH in the flow channel (data kindly provided by Ute Risse-Buhl)

Parameter	Mean ±SD	Parameter	Mean ±SD
Temperature [°C]	7.72 ±1.91	O_2 [mg L^{-1}]	12.06 ±0.91
NO_3-N [mg L^{-1}]	1.26 ±0.46	DOC [mg L^{-1}]	2.25 ±0.63
NH_4-N [mg L^{-1}]	<0.02 ±0.01	TOC [mg L^{-1}]	3.29 ±0.74
NO_2-N [mg L^{-1}]	<0.01 ±0.01	TIC [mg L^{-1}]	15.35 ±1.65
TN [mg L^{-1}]	1.74 ±0.49	conductivity [μS cm^{-1}]	371.4 ±21.4
SRP [mg L^{-1}]	0.01 ±0.00	pH	7.95 ±0.18
TP [mg L^{-1}]	0.03 ±0.00		

3.2.2 Relationship between flow and the turbulent kinetic energy (TKE)

A bell-shaped dependency was observed between the flow velocity and the TKE (Figure 14). At low flow velocities a near streambed turbulence, respectively TKE, occurs. The TKE increases until it peaks at about 0.28 m s^{-1} with a value of 0.0191±0.0014 m^2 s^{-2}. At higher flow velocities, the TKE decreases again until the overall low value of 0.0040±9.58e^{-5} m^2 s^{-2} is reached.
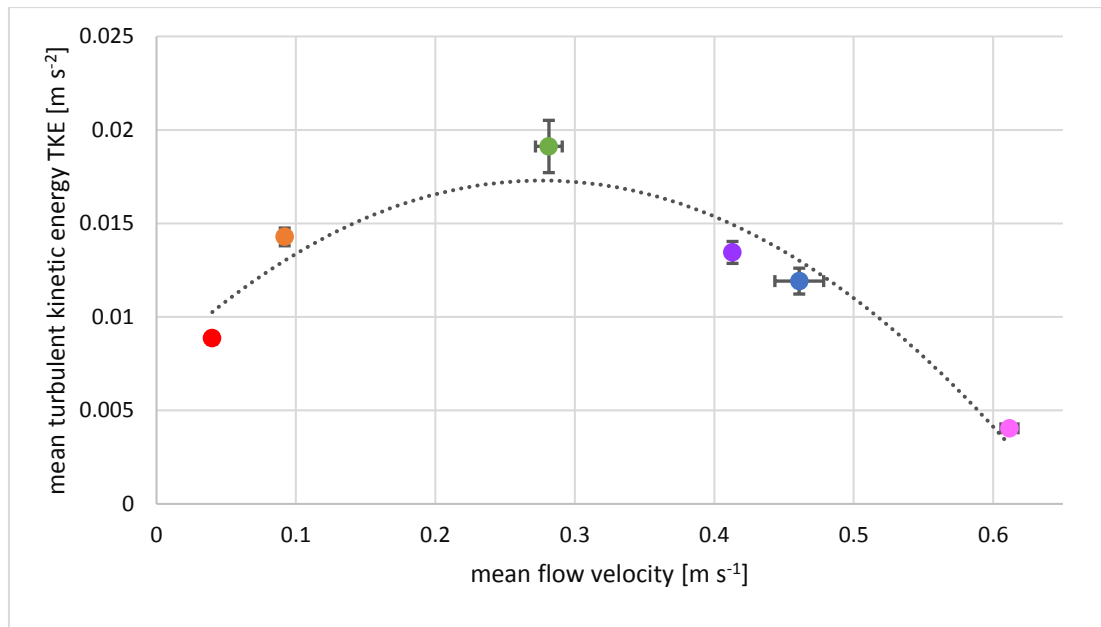
Figure 14: The relationship between the turbulent kinetic energy (TKE) and the mean flow velocity is well represented by a polynomial bell-shaped curve (formula: y = -0.1258x^2 + 0.0695x + 0.0077, R^2=0.915).

3.2.3 Concentration-effect curves and EC50 values of Yield I after exposure to Prometryn

The concentration-effect curves and the EC50-values with their standard error for Yield I after one hour and twenty-four hours of herbicide exposure are shown in figure 15 and table 4. After one hour of herbicide exposure, the sample at the highest flow velocity shows a significant lower EC50 values (8.06±1.90 µmol L^{-1}) and therefore a lower tolerance, respectively a higher sensitivity towards the PSII-inhibiting herbicide Prometryn. A one-way ANOVA-test of the inhibition of Yield I after one hour shows significant differences between the samples for the concentrations 84 µmol L^{-1}, 8.4 µmol L^{-1} and 0.84 µmol L^{-1} ($F_{(5,12)}$=29.4 & 18.6 & 106.5, p<0.001).

After twenty-four hours, the slowest flowing sample B6 (0.04 ±0.0013m s^{-1}) shows a significant lower EC50-value (3.65±0.44 µmol L^{-1}) than the other samples. The residual samples do not differ significantly, partly due to very high standard errors.
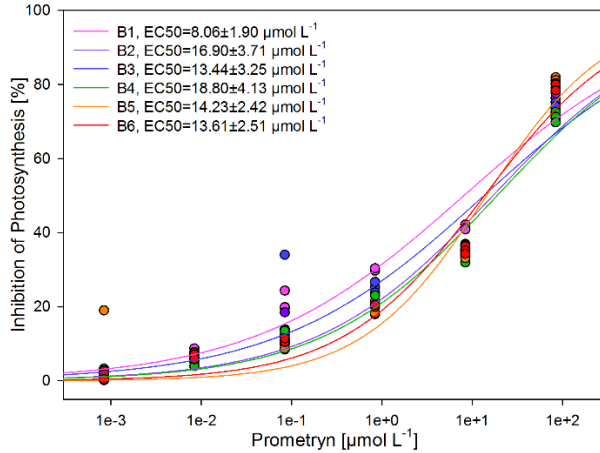
Figure 15: The percental inhibition of the chlorophyll a fluorescence in dependence of the Prometryn concentrations after correcting against the mean values of the DMSO-control is shown for Yield I after one hour of exposure. The EC50-values, which were calculated based on the concentration-effect curves, are displayed together with their standard error.
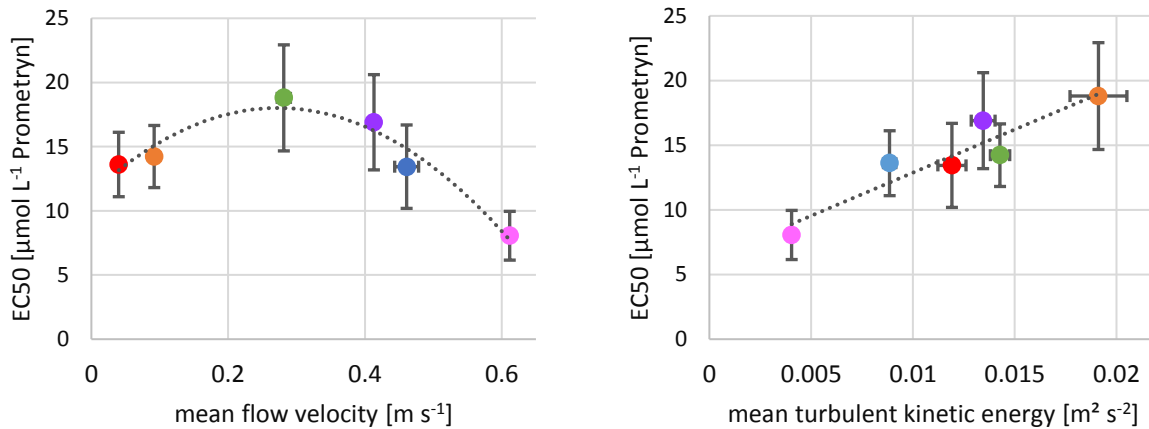
Figure 16: The relationships of the EC50-values of maximum photosynthetic Yield (I) after one hour of exposure with a) the flow velocity (formula: y=-89.66x^2+48.916x+11.341, R²=0.9395) and b) the TKE (formula: y=667.21x+6.2047, R²=0.8702) are shown. Error bars of the hydrological parameters represent the standard-deviation of the averaged values for the two pooled patches. The error bars of the EC50-values represent the calculated standard error after modelling.

The mean EC50-values of Yield I after one hour show a similar bell-shaped relationship towards the mean flow velocity (R²=0.9395) as seen in figure 16a. Comparing the mean EC50-values with

the TKE in figure 16b, a linear correlation can be observed (R^2=0.8702), which is also supported

by the results of the Spearman-test for the mean EC50-values with a $p < 0.05$.

Table 4: The EC50 values and the slope of the Yield (I) measurements shown in figure15 are shown with their respective standard errors (SE) next to the hydrologic parameters and their standard deviation (SD).

Sample	mean flow velocity ±SD [m s^{-1}]	mean TKE ±SD [m^2 s^{-2}]	EC50 ±SE [% µmol^{-1} L^{-1}]	slope ±SE [% µmol^{-1} L^{-1}]
B1	0.61 ±0.01	0.004 ±0.000	8.06 ±1.90	0.37 ±0.03
B2	0.41 ±0.00	0.013 ±0.001	16.9 ±3.71	0.44 ±0.05
B3	0.46 ±0.02	0.012 ±0.001	13.44 ±3.25	0.38 ±0.04
B4	0.28 ±0.01	0.019 ±0.001	18.8 ±4.13	0.45 ±0.05
B5	0.09 ±0.00	0.014 ±0.001	14.23 ±2.42	0.64 ±0.07
B6	0.04 ±0.00	0.009 ±0.000	13.61 ±2.51	0.56 ±0.06

3.2.4 Concentration-effect curves and EC50 values of Yield II after exposure to Prometryn

The concentration-effect curves (figure 17, table 5) show that the inhibition of Yield II after one hour exposure of the fastest flowing sample (0.61±0.0061 m s^{-1}) differs from the other samples. The EC50- value of this sample is with 0.0700±0.0026 µmol L^{-1} significantly lower than the EC50-values of the other samples. A one-way ANOVA-test of the inhibition of Yield II after one hour shows significant differences between the samples for the prometryn concentrations of 0.84 µmol L^{-1} ($p < 0.005$) and 0.084 µmol L^{-1} ($p < 0.001$).

After twenty-four hours of herbicide exposure the samples B2 and B3 show the lowest EC50-values (0.0886±inf & 0.0933±inf µmol L^{-1}). Still, these values do not differ significantly from the others as the standard error for all Yield II samples after twenty-four hours is returned as "infinite" by the software. Furthermore, the inhibition of Yield II after twenty-four hours of the DMSO-control decreases up to 67% compared to the Yield II after one hour and thereby limits the validity of these results.
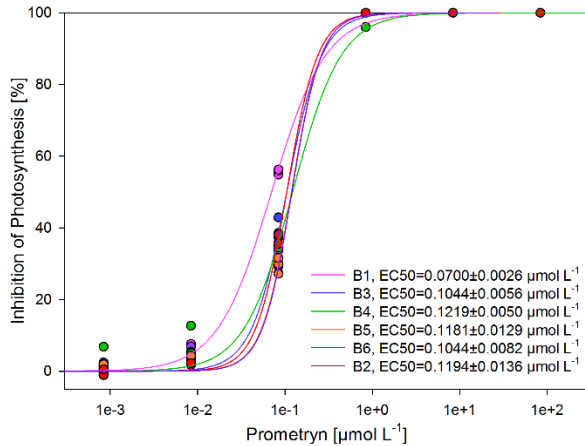
Figure 17: Concentration-effect curves (Hill-model with four parameters) for the measurement of the light-adapted Yield II measurements after a) one hour and b) twenty-four hours. The EC50 values and their standard-error are displayed in the table 5.

The comparison of the mean EC50-values of Yield II after one hour of exposure with the mean flow velocity is shown in figure 18. A bell-shaped polynomial relationship, similar to the one of Yield I, is found (R^2=0.9695). Comparing the mean EC50-values to the mean TKE values, a linear correlation is seen (R^2=0.8288). This linear correlation is proven via the Spearman-test of the respective mean values ($p<0.01$).
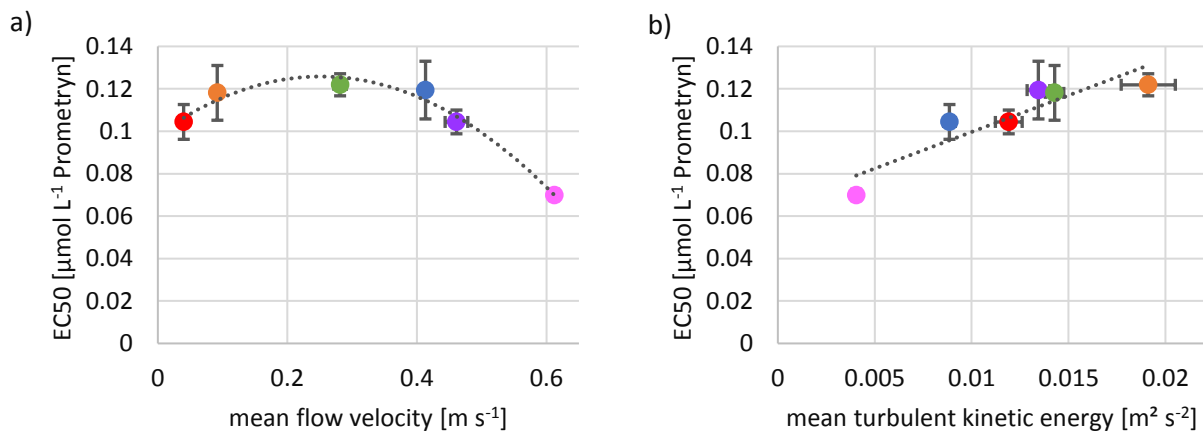
Figure 18: The relationship of the EC50 values of the light-adapted biofilms (Yield II-measurement) after one hour with the mean flow velocity (formula: $y=-0.4312x^2+0.2174x+0.0984$, R^2=0.9395) and the TKE (formula: $y=3.4466x+0.0652$, R^2=0.8288) are shown. Error bars of the hydrological parameters represent the standard-deviation of the averaged values for the two pooled patches. The error bars of the EC50 values represent the calculated standard error.

Table 5: The EC50 values and the slope of the Yield (II) measurements shown in Figure17 are shown with their respective standard errors (SE) next to the hydrologic parameters and their standard deviation (SD).

Sample	flow velocity ±SD [m s^{-1}]	TKE ±SD [m² s^{-2}]	EC50 ±SE [µmol L^{-1}]	slope ±SE [% µmol^{-1} L^{-1}]
B1	0.61 ±0.01	0.004 ±0.000	0.07 ±0.00	1.41 ±0.11
B2	0.41 ±0.00	0.013 ±0.001	0.12 ±0.01	2.56 ±0.87
B3	0.46 ±0.02	0.012 ±0.001	0.10 ±0.01	2.16 ±0.52
B4	0.28 ±0.01	0.019 ±0.001	0.12 ±0.01	1.56 ±0.13
B5	0.09 ±0.00	0.014 ±0.001	0.12 ±0.01	2.54 ±0.86
B6	0.04 ±0.00	0.009 ±0.000	0.10 ±0.01	2.44 ±0.91

3.2.5   Analysis of the diatom community

Overall, 24 taxa were determined in the six samples. The dominating species (>5% share of the community) were *Navicula lanceolata* (Ehrenberg,1838), *Nitzschia ssp.* (presumable mostly *N.palea*) ((Kützing) Smith 1856, *Fistulifera pelliculosa* ((Kützing) Lange-Bertalot 1997), *Adlafia minuscula* ((Grunow) Lange-Bertalot 1999), *Gomphonema oliveacum* (Hornemann & Brèbisson 1838), *Fragilaria recapitellata* (Lange-Bertalot & Metzeltin 2009) and *Surirella brebissonii* (Kramer & Lange-Bertalot 1987). Their relative contribution to the whole community is shown in figure 19, where the 18 taxa with a share below 5% are summed up as "others". The diatom community changes along the gradient of flow velocity. The portion of *Navicula lanceolata* decreases with increasing flow velocity, whereas the portion of *Nitzschia ssp.*, *Fistulifera pelliculosa* and *Adlafia minuscula* increases.
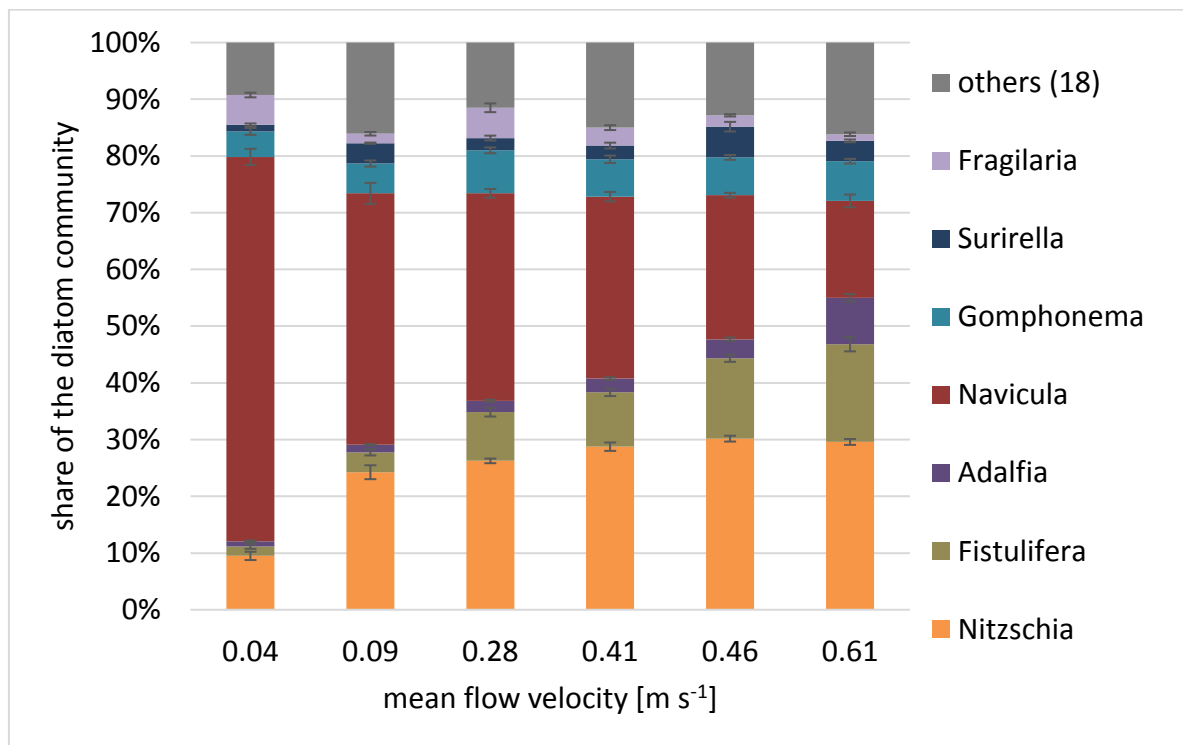
Figure 19: The dominating taxa with a relative abundance of above 5% of the total diatom community are shown, the other eighteen taxa are pooled as "others". Overall twenty-five taxa were found. *Navicula lanceolata* dominates the three slowest-flowing samples (0.04±0.0013 to 0.28 ±0.0096 m s^{-1}). The higher the flow velocity the more equal distributed taxa were found.

The Shannon-Wiener Index, representing the y-diversity, and Evenness, representing the equal distribution of species, show the change of the diatom community along the flow velocity gradient, as well (Figure 20). The Shannon-Wiener Index H_S increases from an average of 1.99±0.06 at 0.04 m s^{-1} to 3.08±0.02 at 0.61 m s^{-1}. Therefore, the ß-diversity increases with flow velocity. At the same time, the evenness E_H increases from an average of 0.48±0.01 to 0.74±0.00 indicating a shift from the dominance of one species, in this case by *Navicula lanceolata*, to a more equal distribution of species. A linear correlation with the TKE was not found (p>0.05).
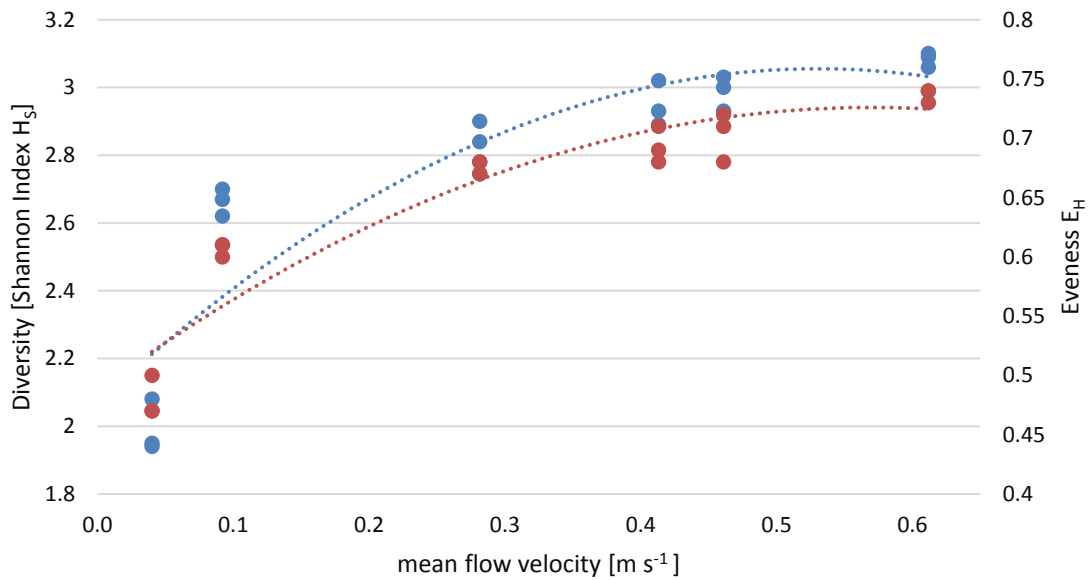
Figure 20: The diversity (blue) on the left y-axis and the evenness (red) on the right y-axis in dependence of the flow velocity are shown. Both increase along the flow velocity with a saturation from xx on. A polynomial relationship is found for both, the diversity (R²=0.8146) and the evenness (R²=0.8811).

A Spearman-test for correlation shows strong correlation of the Shannon-index and the evenness with the mean flow velocity (p<0.01).

3.2.6 Analysis of the extracellular polymeric substances of biofilms

The EPS content in the samples ranges from 113±8 µg cm^{-2} at the sample with the highest flow velocity of 0.61 m s^{-1} (B1) to 458±30 µg cm^{-2} at 0.09 m s^{-1} (B5) (figure 21). Most of the EPS in all samples is build up by carbohydrates, followed by proteins and humic acids. Uronic acids build only a small portion of approximately 5% of the EPS. The ratio of the four fractions shows only small variations between the samples.
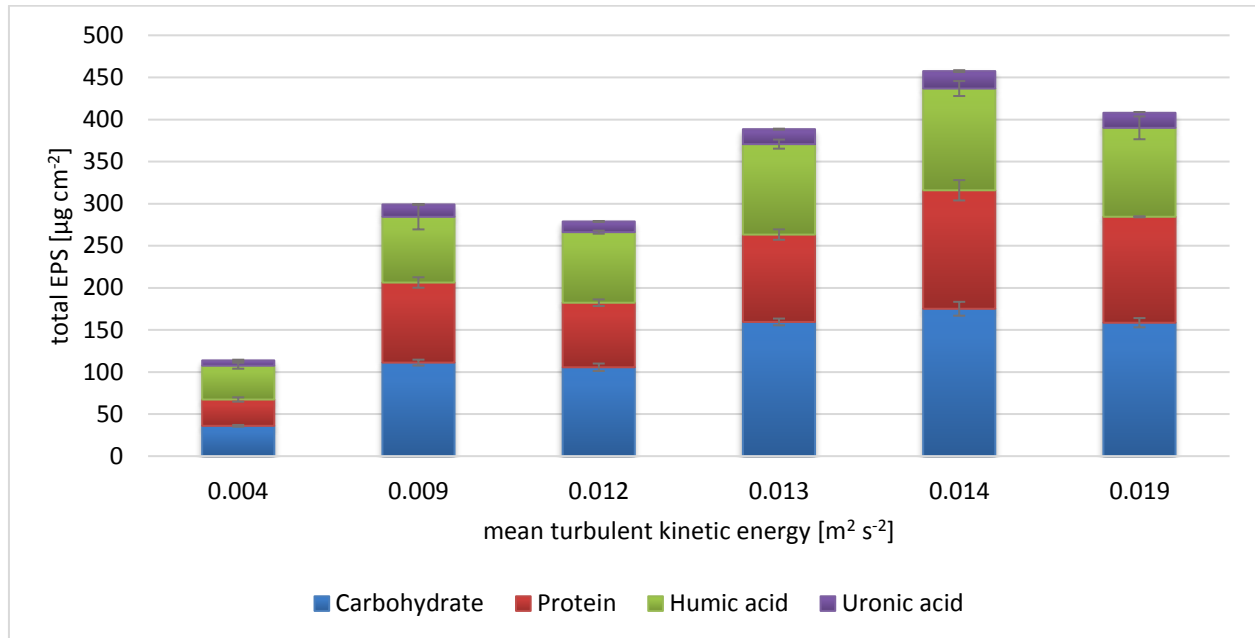
Figure 21: The composition of the EPS matrix of all six samples is given though the four EPS fractions. The carbohydrate fraction has the highest relative portion, closely followed by the Protein and Humic acid fractions. The Uronic acid fraction has the lowest share. The relative portions only differ slightly between the samples.

A linear correlation (R²=0.7125) between the Yield I EC50-values after one hour exposure and the total EPS content is found (figure 22). The significance of the correlation of the respective mean values is supported by the Spearman's test with a p<0.05.
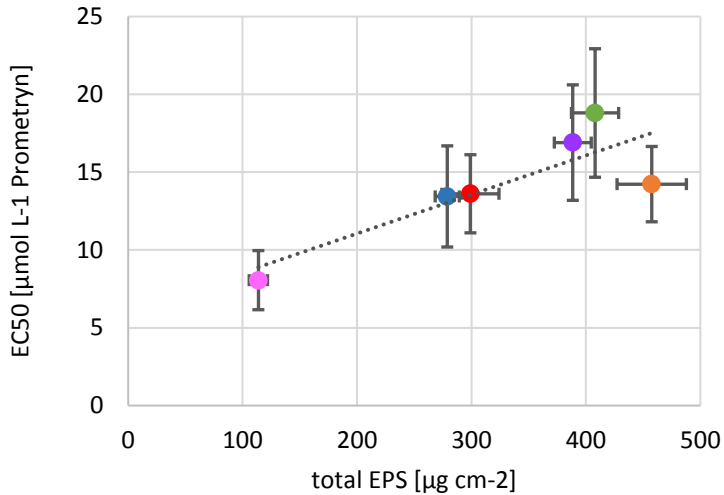
Figure 22:The EC50 values of Yield I after one hour show a linear correlation with the total EPS mass (formula: y=0.0251x+6.0368, R^2=0.7125).

The bell-shaped polynomial relationship (R^2=0.8701) between the mean flow velocity and the total EPS mass mirrors the relationships from the EC50 values of Yield I and Yield II after one hour towards the mean flow velocity (figure 23a). Noteworthy is the decrease from sample B5 (0.014 m^2 s^{-1}) to B6 (0.019 m^2 s^{-1}), where the EPS content differs significantly, although the flow velocity only decreases by 0.05 m s^{-1}. Simultaneously, a linear correlation (R^2=0.7603) of the total EPS mass and the TKE is seen (figure 23b). The significance of the correlations with the total EPS mass are also supported by the Spearman-test, with $p<0.05$ for the EC50 values of both Yields and the TKE.
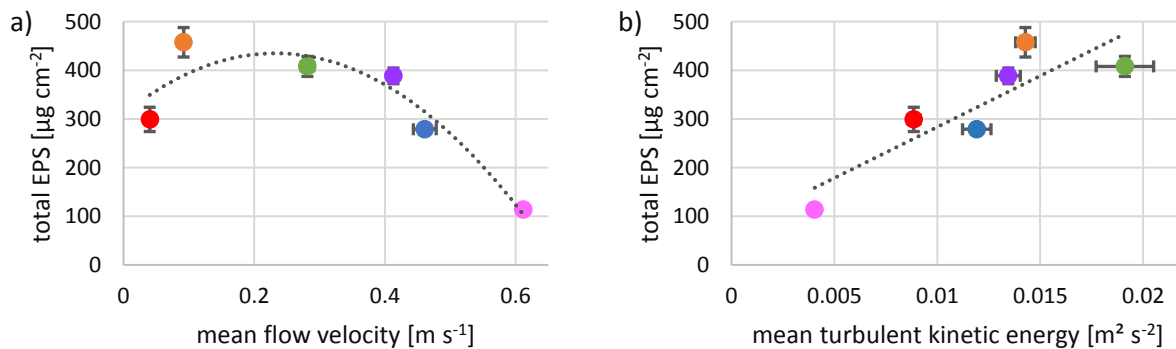
Figure 23: The relationship between the total EPS mass and the a) mean flow velocity and the b) TKE are shown. The total EPS mass has a polynomial correlation with the mean flow velocity (formula: y=-2306.4x^2+1072.9x+310.08, R^2=0.8701) and a linear correlation with the TKE (formula: y=20979x+73.71, R^2=0.7603). The higher the TKE, the higher the total EPS mass.

3.3   Experiment 3: The influence of EPS on the toxicity of Prometryn

In a follow-up experiment the new hypothesis, which was derived from the flow channel experiment, was tested, namely, that the EPS matrix absorbs the herbicide and inhibits its effect. This hypothesis was tested with artificial EPS based on the EPS-contents of the biofilms from the flow channels. The concentration-effect curves for the artificial EPS show a clear trend and significant differences in their EC50 values at Yield I after one hour (figure 24). The higher the added EPS concentration to the sample the higher is the EC50 value of the *Nitzschia palea* biofilm.
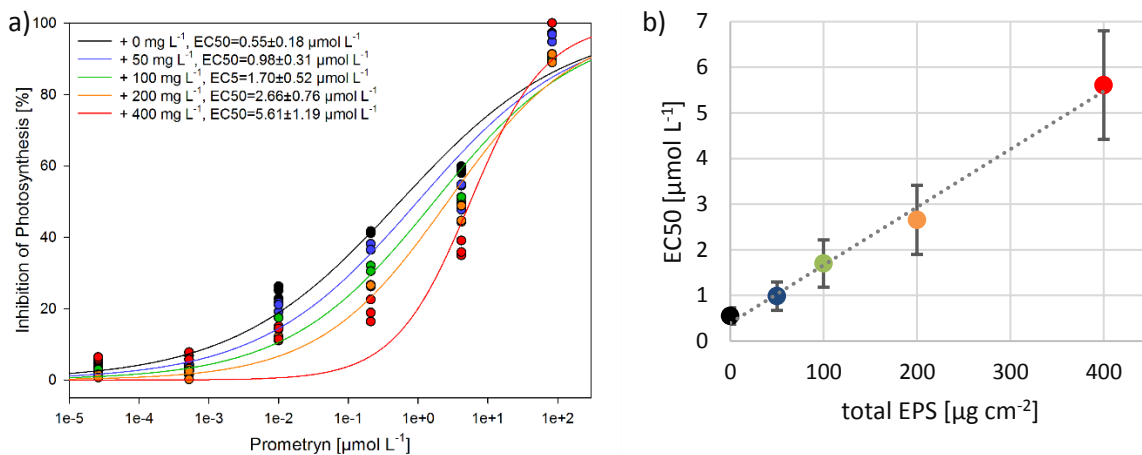
Figure 24: a) The concentration-effect curve (Yield I) for the additional mixed-EPS shows differences in the four treatments. The EC50-values of the different treatments are shown in the legend. b) The mass of the additional EPS correlates significantly with the EC50 values of the dark-adapted Yield I after one hour (formula: y=0.0127x+0.3956, R^2=0.9924).

The EC50 values of Yield I after one hour of prometryn exposure also show a strong correlation (R^2=0.9924) with the sum of additional DOC, respectively artificial EPS. The same trend at Yield I is still visible after twenty-four hours, but the EC50 values for 50 and 100 mg L^{-1} and the EC50 values for 200 and 400 mg L^{-1} do not differ significantly anymore. No such trend or correlation is found for Yield II after one hour exposure, but for the twenty-four hour exposure (R^2=0.8355). The EC50 values of the treatments with the artificial EPS for Yield II after twenty-four hours differ significantly, but are all placed within the modeled standard error of the zero control.

A one-way ANOVA-test between the different groups of additional EPS shows significant ($p<0.05$) differences for all Prometryn concentrations except of 83.2 µmol L^{-1}.
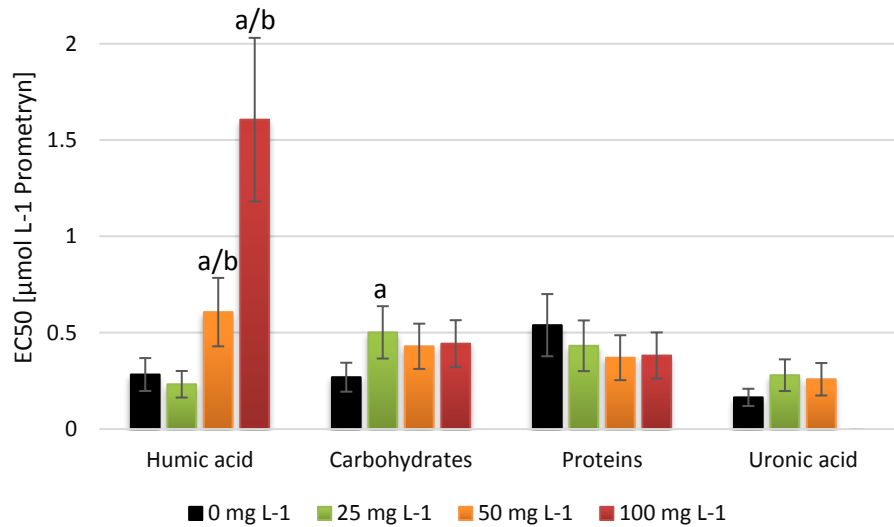
Figure 25: The EC50-values derived from the inhibition of Yield I after one hour are shown for each treatment of the four EPS fractions. The EC50-value for the 100 mg L^{-1} treatment of uronic acid is missing, as the software could not calculate it due to an unkown error. Significant differences to the control (+0 mg L^{-1}) are marked with an "a", significant differences towards the next lower concentration are marked with a "b" .

The herbicide assays that were conducted to examine which of the EPS groups influence the concentration-effect curves (figure 25), show that humic acids influence both photosynthetic Yields at both time points (one and twenty-four hours of exposure, respectively). While the addition of 25 mg L^{-1} humic acid does not show a significant difference of the EC50-values, the treatments with 50 mg L^{-1} and 100 mg L^{-1} show a significant increase of the EC50-value. Thus, the addition of 50 mg L^{-1} and 100 mg L^{-1} decreases the toxicity of Prometryn. The other fractions (Proteins: bovine serum albumin; Uronic acids: Glucuronic acid) show no significant increase of the EC50-value along the gradient of additional EPS. While the EC50-values of the biofilms for Carbohydrates and Uronic acid with the additional EPS are higher than the treatment without (+0 mg L^{-1}), there is no overall significant increase within the treatments. For the Protein treatment, the biofilms without additional Protein-EPS shows the highest EC50-value and no significant change with increasing additional EPS.

4 Discussion

4.1 Comparison of attached and suspended biofilms

The results of our study show differences in the herbicide sensitivity between the attached and the suspended biofilm for both yields. The attached biofilms are less sensitive towards herbicides than suspended biofilms. Scratching off and suspending biofilms for further measurements is common practice (Dorigo *et al.*,2010; Lambert *et al.*,2015). Still, attached biofilms are also used but less frequent (Guasch *et al.*,2003; Tlili *et al.*,2011). Patil & Anil (2005) discusses the use of different methods of scratching off for the quantification of diatoms and favors the use of nylon brushes to prevent underestimation.

The only known study, comparing herbicide sensitivity of attached and suspended biofilms, respectively recolonized, biofilms was conducted by Paule *et al.* (2013). They conclude that "[…] there was no evidence on the role of the biofilm as a barrier to alachlor" (Paule *et al.*,2013). Contrasting to this, Flemming (1993) reviews that the "biofilm mode of growth" protects against toxic substances. Therefore, our results confirm the protective role of the biofilm formation. Another parameter that needs to be considered is the biofilm thickness, as increasing thickness correlates positively with the time scale needed for equilibration of dissolved organic contaminants between the water column and within biofilms (Wicke *et al.*,2008). Overall, our results show that the absolute EC50-values of studies conducted with suspended biofilms are approx. three to four times overestimated compared to attached biofilms. Still, the slope does not differ and indicates an equal bioavailability for both biofilm states.

Stream biofilms build up different internal structures, e.g. channels, to increase their nutrient availability (Biggs and Smith,2002; Stoodley *et al.*,2002). These structures, which may influence the bioavailability of the herbicides, get destroyed when the biofilms are scratched off. Using suspended biofilms increases the chance of contact between the herbicide and the single algae cells and therefore the bioavailability. Nevertheless, the use of suspended biofilms shows an advantage, as the deviation of the yield measurements of the samples is more uniform due to the homogenization.

The measurements of the yield of the chlorophyll fluorescence, the algae classes determined with the Phyto-PAM fluorometer and the algae-associated pigments differ before and after scratching off the biofilms. At the algae classes only the percental abundance of cyanobacteria differs significantly and at the pigment analysis the Chlorophyll a, Fucoxanthin and Beta-Carotene decreased significantly. This may be caused by the loss of biomass during the process of scratching off and resuspending. Further an increased degradation of these pigments due to damaging the cells and causing a cell-lysis may be possible.

It remains to be noted that the use of scratched off and suspended biofilms leads to changes in the absolute values of the measured structural and functional parameters but also decrease heterogeneity and thereby increases the distinctness of the measurements. Still, suspended biofilms have the practical advantages of a faster processing of a higher volume at a lower heterogeneity.

4.2   Flow velocity and turbulent kinetic energy

The relationship between the mean flow velocity and the TKE in this study is well described by a bell-shaped curve. In gravel bed streams, mean flow velocity is often correlated with turbulent intensity and turbulent flow structure properties, as when mean flow velocity increases also turbulence tends tend to increase (Nikora,2007). However, due to the use of noozles which created the jet-like flow, the correlations between flow velocity and turbulence deviated from natural stream systems. While this flaw decreases the correct reflection of the natural system, it allows in the following to clearly differentiate, which of the two hydrodynamic parameters causes differences of the herbicide tolerance.

Other inferences that may limit the measurements or the outcome of this study are possible edge effects near the vertical walls of the flow channel and the even level of the substrate, which does not reflect the natural system correctly.

4.3   Herbicide tolerance of the biofilms under differing hydrodynamic conditions

The herbicide tolerances correlate with the near streambed turbulence (TKE) but not with the flow velocity. Former studies about hydrodynamic influences focused on flow velocities and their effect on structural and functional parameters of biofilms: Villeneuve *et al.* (2011) found that an

increasing flow velocity has a positive effect on primary production, algal density, bacterial production and bacterial density. This may be caused by an increased retention of nutrients by the biofilm at high flow velocities (Biggs and Hickey,1994; Villeneuve *et al.*,2011). In a follow up study, Villeneuve *et al.* (2011) tried to link these structural and functional differences to possible differences in herbicide tolerance. But they found no correlation of the EC50-values and the flow velocity. They concluded that the EC50-values of the pooled samples of a turbulent flow channel are lower than the one of the laminar flow channel. This indicates that the turbulence has an influence on the herbicide tolerance, respectively sensitivity, and not the flow velocity per se. In a recent study conducted at the River Selke and the nearby River Kalte Bode, Risse-Buhl *et al.* (2017) highlighted the role of the near streambed turbulence on the composition and architecture of stream biofilms. The algal biovolume as well as the surface coverage increased with near streambed turbulence indication that biofilms spreading more uniformly on the mineral surface.

The missing link between the flow velocity and the herbicide tolerance described in Villeneuve *et al.* (2011) is confirmed in this study. Furthermore, based on the recently highlighted role of the near streambed turbulence on epilithic stream biofilm structure (Risse-Buhl *et al.*,2017) and the lower herbicide tolerance in the turbulent flow channel found by Villeneuve, a correlation between the near streambed turbulence and the herbicide tolerance of stream biofilms, as found in this study, replace this missing link, as the near streambed turbulence is the crucial hydrodynamic parameter for the herbicide tolerance. This connection is highlighted though this study.

Therefore, an additional aim of this study was to mechanistically understand hydrodynamic-induced changes in biofilms which might be relevant for the tolerance of biofilms to herbicides. Two hypotheses are discussed in the following: (1) hydrodynamic-induced changes in community composition and (2) changes in the EPS-content of biofilms.

4.4 Diatom community along a gradient of flow velocity

A clear trend in the diversity and evenness of the diatom community is observed, both diversity parameters (Shannon-Weaver index & Evenness) correlate positively with increasing flow velocity. The TKE does not play a role hereby. The increase along an increasing flow velocity is contradictory to other studies. So found Soininen (2004) a decrease in the diatom diversity

(Shannon-Weaver index) over a gradient of three flow velocities (10, 40 and 100 cm s^{-1}). Villeneuve *et al.* (2011) concludes that the heterogeneity of hydrological conditions increases the overall biodiversity, but cannot correlate the biodiversity with a gradient of these conditions.

Even though Passy (2007) used a morphology-based guild approach instead of determination of unique taxa, she found an increase in guild diversity, respectively guild evenness, (motile, low- and high-profile) with increasing flow velocity. The guild diversity peaks at 0.45 m s^{-1} and decreases only slightly at higher flow velocities which is corresponding to the findings of this study. All taxa found in our samples can be assigned to certain morphology-based genera guilds proposed by Passy (2007); Passy (2017)and Wu *et al.* (2017). Overall, the share of the motile guild is the highest and decreases from 77.4±3.2% at 0.04 m s^{-1} to 47.8±3.7% at 0.61 m s^{-1} (see annex V). At the same time, the high-profile guild increases from 7.1±1.8% to 18.6±1.3% and the low-profile guild decreases slightly from 6.0±1.5% to 4.0±1.1%. Unlike Passy (2007), where the motile guild stays on a constant low level, it has the highest share in our samples and decreases with increasing flow velocity. The trends of the other two guilds are also contradictory to the results in Passy (2007). The low share of the low-profile guild may be explained by the self-shading within biofilms (Passy 2007).

Focusing more on the species-specific preferences for certain flow velocities, *Navicula lanceolata* shows the highest share at the lowest flow velocity. All further addition, respectively increase, of other species outcompete this single species, which is contradictory to the results of other authors. Biggs & Hickey (1994) found no change in the dominating species along a flow velocity gradient from 0.1 to 1.5 m s^{-1}. The distribution of the diatoms also may reflect the outcome of competition (Mulder *et al.*,2001; Cardinale and Palmer,2002; Passy,2017). While the lower end of the flow velocity gradient was probably driven by competition, the higher end was probably dominated by the disturbance stress of the high flow velocity (Hondzo and Wang,2002). Therefore, one dominating species may "wins" the competition at low disturbances but couldn't succeed at higher disturbances, respectively flow velocities. In our case, it seems to be the other way around. *Navicula lanceolata* "wins" the competition at relative undisturbed conditions with a low flow velocity but loses against other species the higher the flow velocity gets.

Furthermore, only one species found in our study can be assigned a specific preferred flow velocity. Ghosh & Gaur (1998) found that *Gomphonema oliveacum* favors flow velocities of 0.18 to 0.21 m s^{-1} in a community biofilm experiment. This result cannot be confirmed in our study, as *G. oliveacum* appears at a constant share of the community throughout the different flow velocities.

Looking at diatoms in a more general view, Arnon *et al.* (2007) found that the share of diatoms increases with increasing flow velocity compared to green algae and cyanobacteria. This decrease opens more niches for diatoms as competing non-diatom species vanish. This may additionally explain the increase of diatom taxa.

Still, the correlation of diatom diversity and flow velocity can barely explain the increase in biofilm tolerance to toxicants and needs more investigation beyond our study.

4.5   Herbicide sensitivity of the diatom community

Reviewing the herbicide sensitivity of the single taxa level, only spare information can be found. Roubeix *et al.* (2011) lists the EC50 values of *Navicula lanceolata* and *Nitzschia palea* towards the PSII-inhibition herbicide Diuron. While we cannot compare the absolute EC50-values of the single species in Roubeix *et al.* (2011) towards the EC50-values of the biofilm communities in this study, due to the use of different herbicides, a comparison of a general trend seems reliable. While *Navicula lanceolata* shows an EC50-value of 6.8±0.8 µg L^{-1}, the EC50-value of *Nitzschia palea* is about three-fold higher (18.5±1.7 µg L^{-1}) in monoculture. Applied on the results of our study, where *Navicula lanceolata* is more abundant in samples with higher EC50-values, contradictory results would have been expected, when the trend in the EC50-values could be explained by the sensitivity of the single species. Due to the fact that data for other species are missing, that other algae classes but diatoms are expected to be present in the samples as well, and the missing statistical link of the flow velocity towards the EC50-values, it seems very likely, that the species composition of the biofilm community does not cause the differences in the EC50-values within the experiment of this study

Considering the diversity itself, the "biological insurance hypothesis" (Yachi and Loreau,1999) applied on biofilms suggests that biofilms with a higher diversity would be less sensitive towards

herbicides. This hypothesis was tested by Villeneuve *et al.* (2011) and could not be proofed. Instead Villeneuve *et al.* (2011) found that biofilms with a higher diversity from a heterogeneous turbulent flow channel were more sensitive to herbicides than less diverse biofilms from a homogenous laminar flow channel. This indicates either that taxa occurring at turbulent conditions have a lower EC50, which could not be proofed in our study, or that something else, e.g. the EPS matrix, plays a role for the herbicide sensitivity. We found that biofilms that are exposed to less stress in form of the TKE are more sensitive towards herbicides. Thus, our results are contrasting to the hypothesis by Yachi & Loreau (1999). Therefore, another cause may have a stronger influence on the herbicide sensitivity than the sensitivity of single taxa or the biodiversity itself.

4.6   The EPS matrix along the TKE

The total EPS matrix correlates with the near streambed turbulences (TKE) but not with the flow velocity. The biofilm matrix, which is build up by extracellular polymeric substances, plays an important role for the organisms in biofilms and the biofilm structure itself. Next to the nutrient supply, the influence of hydrological conditions is well assessed in literature. Battin *et al.* (2003a) compared stream biofilms at two different flow velocities (0.065 ± 0.011 m s^{-1} & 0.23 ± 0.02 m s^{-1}), respectively shear stress (1.07 ± 0.26 & 13.31 ± 0.48 N m^{-2}), and found higher biofilm thickness and density under slower flow velocities. Battin *et al.* (2003a) did not find significant differences in the EPS content per area, but found significant differences in the EPS content per cell. Unlike Battin *et al.* (2003a), Biggs & Hickey (1994) found a higher mucilage content at higher flow velocities. Looking at the microscopic structure of biofilms, Battin *et al.* (2003a) found structural patterns of the EPS parallel to the flow velocity at higher velocities. Quasi-hexagonal structures found at higher flow velocities, respectively shear stress, increases the stability of the biofilms. Contrasting to Battin *et al.* (2003a) results, Risse-Buhl *et al.* (2017) found a decrease of the biovolume to EPS ratio with increasing near streambed turbulences (represented by the TKE), which is eventually caused by the use of an insufficient EPS-staining fluorescent for EPS determination. Wang *et al.* (2014) used a similar approach as in our study to determine the EPS content and found a higher EPS content, respectively density, in thinner biofilms at higher flow velocities (0.28 m s^{-1}) as in

thicker biofilms from slower flow velocities (0.01 m s^{-1}). Although the biofilm thickness was not measured in our study, a correlation between the EPS content and the TKE was found. While the thickness is not an appropriate measure for the EPS itself due to flow-velocity depending densities, our results match the results for the total EPS mass from Wang *et al.* (2014). There is no study so far investigating the role of the total EPS and the near streambed turbulence. Synthesizing, based on the results by Risse-Buhl *et al.* (2017) and Wang *et al.* (2014), it can be concluded that higher near streambed turbulences induce a higher EPS content in biofilms.

4.7   EPS absorption of herbicides

The results of the EPS analysis show a linear correlation with the EC50-values of the herbicide assay. The results of the absorption experiment with the artificial EPS highlight the role of humic acids on the absorption of herbicides. Former studies in soils have shown the absorbing effect of DOM, respectively organic carbon, on herbicide effects (Baskaran and Kennedy,1999; Ling *et al.*,2006). The role of humic substances is highlighted in literature (Bollag and Myers,1992; Senesi,1992) and confirmed by the results of our final experiment. Furthermore, Bollag & Myers (1992) described the binding mechanism of herbicides to extracellular enzymes. Even though we didn't quantify them in our study, extracellular enzymes are highly abundant in the EPS matrix of biofilms (Flemming and Wingender,2010). Lawrence *et al.* (2001) have already proven the accumulation of herbicides in the EPS matrix of attached stream biofilms but did not examine whether this changes their bioavailability and did not relate this finding to toxic effects. However, it needs to be considered that the absolute values of the EPS mass of the flow-channel experiment in our study may be overestimated, due to possible cell lysis during the EPS extraction (Takahashi *et al.*,2009; Wang *et al.*,2014). Therefore, the decrease in toxicity of prometryn through increasing artificial EPS was proven by a confirmation experiment.

4.8   Actual role of the EPS matrix for biofilms and behaviour towards herbicides

As the biofilm matrix acts primarily "as an external digestive systems […]" (Flemming and Wingender,2010) and not specifically as a barrier towards herbicides, it is necessary to understand, why the mass of the EPS matrix increases with increasing TKE, respectively flow velocity. Augspurger & Küsel (2010) found, without measuring near streambed turbulences, that

the carbon uptake of nascent stream biofilms is fostered by higher flow velocities. Risse-Buhl *et al.* (2017) states that a high TKE enhances mass transport and eventually affects retention and transformation of carbon and nutrients in mature stream biofilms. Biggs & Hickey (1994) found that biofilms increase their density to resist the shear stress although, the higher EPS content may limit their mass transport rate, respectively the diffusivity (Beyenal and Lewandowski,2002). At lower densities biofilms increase their access to nutrients by incorporating channels in their structure which are missing in denser biofilms (Stoodley and Lewandowski,1994; Stoodley *et al.*,1997).

These adaptions, which were primarily evolved for higher nutrient availability, may work the same for pollutants. Lawrence *et al.* (2001) has shown that biofilms can accumulate and metabolize herbicides. But it is not known, if this mechanism increases or decreases the bioavailability and therewith toxicity of the herbicide towards the biofilm organisms. As our study was conducted in a catchment with low anthrophonic impact, respectively herbicide contamination, the biofilms did not come up with structural or functional adaptions towards herbicides. This indicates that the effect of co-tolerance of biofilms in different near streambed turbulences towards acute herbicide exposure is very likely an unintended mechanism. The mechanistic interaction of the different structural adaptions towards different hydrologic regimes needs to be considered in future experiments. In our study, we only focused on the total EPS mass as the biofilms were scratched off and suspended.

On a larger scale this means that biofilms in rivers are more sensitive towards herbicides when the biofilms experience low near-streambed turbulences. In hydrodynamic altered rivers this likely is the case and the two stressors, hydrologic alteration and herbicide pollution, create an antagonistic effect which affects the stream biofilms heavily.

4.9   Conclusion

-   The flow velocity shapes the species-distribution within biofilms. The diatom diversity increases with increasing flow velocity.

-   Differences in the near-streambed turbulences induce different manifestation of the EPS matrix. The higher the TKE, the higher the EPS content. The EPS matrix then plays a major role for the absorption and bioavailability of herbicides to the biofilm microbes.

-   Especially, humic acids are able to absorb herbicides and inhibit their effect on biofilm microbes. In general, complex structures, e.g. extracellular enzymes, are thought to absorb herbicides more efficiently.

-   The herbicide sensitivity of biofilms is indirectly depending on the near streambed turbulences, but not on the flow velocities.

References

Arnaud, L., G. Taillandier, M. Kaouadji, P. Ravanel and M. Tissut (1994). "Photosynthesis Inhibition by Phenylureas: A QSAR Approach." Ecotoxicology and Environmental Safety 28(2): 121-133.

Arnon, S., A. I. Packman, C. G. Peterson and K. A. Gray (2007). "Effects of overlying velocity on periphyton structure and denitrification." Journal of Geophysical Research-Biogeosciences 112(G1): 10.

Augspurger, C. and K. Küsel (2010). "Flow velocity and primary production influences carbon utilization in nascent epilithic stream biofilms." Aquatic Sciences 72(2): 237-243.

Barranguet, C., S. A. M. van Beusekom, B. Veuger, T. R. Neu, E. M. M. Manders, J. J. Sinke and W. Admiraal (2004). "Studying undisturbed autotrophic biofilms: still a technical challenge." Aquatic Microbial Ecology 34(1): 1-9.

Baskaran, S. and I. R. Kennedy (1999). "Sorption and desorption kinetics of diuron, fluometuron, prometryn and pyrithiobac sodium in soils." Journal of Environmental Science and Health, Part B 34(6): 943-963.

Battin, T. J., K. Besemer, M. M. Bengtsson, A. M. Romani and A. I. Packmann (2016). "The ecology and biogeochemistry of stream biofilms." Nat Rev Micro 14(4): 251-263.

Battin, T. J., L. A. Kaplan, J. D. Newbold, X. H. Cheng and C. Hansen (2003a). "Effects of current velocity on the nascent architecture of stream microbial biofilms." Applied and Environmental Microbiology 69(9): 5443-5452.

Battin, T. J., L. A. Kaplan, J. D. Newbold and C. M. E. Hansen (2003b). "Contributions of microbial biofilms to ecosystem processes in stream mesocosms." Nature 426(6965): 439-442.

Bertzen, G. and R. Müller (2002). "Diatomeen: Präparation und Ökologie." Ökologische Station Sorpesee.

Beyenal, H. and Z. Lewandowski (2002). "Internal and External Mass Transfer in Biofilms Grown at Various Flow Velocities." Biotechnology Progress 18(1): 55-61.

Biggs, B. J. F. and C. W. Hickey (1994). "Periphyton responses to a hydraulic gradient in a regulated river in New Zealand." Freshwater Biology 32(1): 49-59.

Biggs, B. J. F., V. I. Nikora and T. H. Snelder (2005). "Linking scales of flow variability to lotic ecosystem structure and function." River Research and Applications 21(2-3): 283-298.

Biggs, B. J. F. and R. A. Smith (2002). "Taxonomic richness of stream benthic algae: Effects of flood disturbance and nutrients." Limnology and Oceanography 47(4): 1175-1186.

Blanck, H., S.-Å. Wängberg and S. Molander (1988). Pollution-induced community tolerance—a new ecotoxicological tool. Functional testing of aquatic biota for estimating hazards of chemicals, ASTM International.

Blumenkrantz, N. and G. Asboe-Hansen (1973). "New method for quantitative determination of uronic acids." Analytical Biochemistry 54(2): 484-489.

Bollag, J.-M. and C. Myers (1992). "Detoxification of aquatic and terrestrial sites through binding of pollutants to humic substances." Science of The Total Environment 117-118(Supplement C): 357-366.

Busch, W., S. Schmidt, R. Kühne, T. Schulze, M. Krauss and R. Altenburger (2016). "Micropollutants in European rivers: A mode of action survey to support the development of effect-based tools for water monitoring." Environmental Toxicology and Chemistry 35(8): 1887-1899.

Cardinale, B. J. and M. A. Palmer (2002). "Disturbance moderates biodiversity-ecosystem function relationships: Experimental evidence from daddisflies in stream mesocosms." Ecology 83(7): 1915-1927.

de Brébisson, A. (1838). Considérations sur les Diatomées, et essai d'une classification des genres et des espèces appartenant a cette famille, Brée.

DeLorenzo, M. E., G. I. Scott and P. E. Ross (2001). "Toxicity of pesticides to aquatic microorganisms: A review." Environmental Toxicology and Chemistry 20(1): 84-98.

DIN EN ISO 11732-E32 (2005), Water Quality - Determination of Ammonium Nitrogen - Method by Flow Analysis (CFA and FIA) and Spectrometric Detection (E23), Berlin, Beuth

DIN EN ISO 11905-1-H36 (1998), Water Quality - Determination of Nitrogen - Part 1: Method Using Oxidative Digestion with Peroxodisulfate (H36), Berlin, Beuth

DIN EN ISO 13395-D28 (1996), Water Quality - Determination of Nitrite Nitrogen and Nitrate Nitrogen and the Sum of Both by Flow Analysis (CFA and FIA) and Spectrometric Detection (D28), Berlin, Beuth

DIN EN ISO 15681 Part 2-D46 (2005), Water Quality - Determination of Orthophosphate and Total Phosphorus Contents by Flow Analsysis (FIA and CFA) - Part 2: Method by Continuous Flow Analysis (CFA) (D46), Berlin, Beuth

DIN 38405-11 (1983), German Standard Methods for the Examination of Water, Waste Water and Sludge; Anions (Group D); Determination of Phosphorus Compounds (D 11), Berlin, Beuth

Dorigo, U., A. Berard, F. Rimet, A. Bouchez and B. Montuelle (2010). "In situ assessment of periphyton recovery in a river contaminated by pesticides." Aquatic Toxicology 98(4): 396-406.

DuBois, M., K. A. Gilles, J. K. Hamilton, P. t. Rebers and F. Smith (1956). "Colorimetric method for determination of sugars and related substances." Analytical chemistry 28(3): 350-356.

EEA (2012). European Waters: Assessment of Status and Pressures, European Environment Agency.

Ehrenberg, C. G. (1838). "Infusionsthierchen als vollkommene Organismen: ein Blick in das tiefere organische Leben der Natur."

Eßer, M. (2006). Long-term dynamics of microbial biofilm communities of the river Rhine, Universität zu Köln.

Flemming, H.-C. (1993). "Biofilms and environmental protection." Water Science and Technology 27(7-8): 1-10.

Flemming, H.-C. and J. Wingender (2010). "The biofilm matrix." Nat Rev Micro 8(9): 623-633.

Frolund, B., T. Griebe and P. H. Nielsen (1995). "Enzymatic activity in the activated-sludge floc matrix." Applied Microbiology and Biotechnology 43(4): 755-761.

Fuerst, E. P. and M. A. Norman (1991). "Interactions of Herbicides with Photosynthetic Electron Transport." Weed Science 39(3): 458-464.

G. H. Krause, E. W. (1991). "Chlorophyll Fluorescence and Photosynthesis: The Basics." Annual Review of Plant Physiology and Plant Molecular Biology 42(1): 313-349.

Genty, B., J.-M. Briantais and N. R. Baker (1989). "The relationship between the quantum yield of photosynthetic electron transport and quenching of chlorophyll fluorescence." Biochimica et Biophysica Acta (BBA) - General Subjects 990(1): 87-92.

Ghosh, M. and J. P. Gaur (1998). "Current velocity and the establishment of stream algal periphyton communities." Aquatic Botany 60(1): 1-10.

Graba, M., S. Sauvage, F. Y. Moulin, G. Urrea, S. Sabater and J. M. Sanchez-Perez (2013). "Interaction between local hydrodynamics and algal community in epilithic biofilm." Water Research 47(7): 2153-2163.

Guasch, H., W. Admiraal and S. Sabater (2003). "Contrasting effects of organic and inorganic toxicants on freshwater periphyton." Aquatic Toxicology 64(2): 165-175.

Guasch, H., I. Muñoz, N. Rosés and S. Sabater (1997). "Changes in atrazine toxicity throughout succession of stream periphyton communities." Journal of Applied Phycology 9(2): 137-146.

Guiry, M. D. and G. M. Guiry. (2017). "AglaeBase." Retrieved 01.08.2017, from http://www.algaebase.org/.

Hofmann, G., M. Werum and H. Lange-Bertalot (2013). Diatomeen im Süßwasser–Benthos von Mitteleuropa. Bestimmungsflora Kieselalgen für die ökologische ökologische Praxis. Über 700 der häufigsten Arten und ihre Ökologie, Koeltz Scientific Books, Koenigstein.

Hondzo, M. and H. Wang (2002). "Effects of turbulence on growth and metabolism of periphyton in a laboratory flume." Water Resources Research 38(12): 9.

Kelly, M. G., H. Bennion, E. J. Cox, G. Goldsmith, J. Jamieson, S. Juggins, D. G. Mann and R. J. Telford. (2005). "Common freshwater diatoms of Britain and Ireland: an interactive key." Retrieved 01.08.2017, from http://craticula.ncl.ac.uk/EADiatomKey/html/index.html.

Kintner, P. K. and J. P. Van Buren (1982). "Carbohydrate Interference and Its Correction in Pectin Analysis Using the m-Hydroxydiphenyl Method." Journal of Food Science 47(3): 756-759.

Krammer, K. and H. Lange-Bertalot (1987). "Morphology and taxonomy of Surirella ovalis and related taxa." Diatom Research 2(1): 77-95.

Labiod, C., R. Godillot and B. Caussade (2007). "The relationship between stream periphyton dynamics and near-bed turbulence in rough open-channel flow." Ecological Modelling 209(2): 78-96.

Lambert, A. S., S. Pesce, A. Foulquier, J. Gahou, M. Coquery and A. Dabrin (2015). "Improved short-term toxicity test protocol to assess metal tolerance in phototrophic periphyton: toward standardization of PICT approaches." Environmental Science and Pollution Research 22(6): 4037-4045.

Lange-Bertalot, H. (1997). "Frankophila, Mayamaea und Fistulifera: drei neue Gattungen der Klasse Bacillariophyceae." Archiv für Protistenkunde 148(1-2): 65-76.

Lange-Bertalot, H. (1999). "Diatoms from Siberia I. Islands in the Arcic Ocean (Yugorsky Shar Strait)." Iconographia Diatomologica 6: 273.

Larned, S. T. (2010). "A prospectus for periphyton: recent and future ecological research." Journal of the North American Benthological Society 29(1): 182-206.

Larned, S. T., V. I. Nikora and B. J. F. Biggs (2004). "Mass-transfer-limited nitrogen and phosphorus uptake by stream periphyton: A conceptual model and experimental evidence." Limnology and Oceanography 49(6): 1992-2000.

Lau, Y. L. and D. Liu (1993). "Effect of flow-rate on biofilm accumulation in open channels." Water Research 27(3): 355-360.

Lawrence, J. R., G. Kopf, J. V. Headley and T. R. Neu (2001). "Sorption and metabolism of selected herbicides in river biofilm communities." Canadian Journal of Microbiology 47(7): 634-641.

Ling, W., J. Xu and Y. Gao (2006). "Dissolved organic matter enhances the sorption of atrazine by soil." Biology and Fertility of Soils 42(5): 418-425.

Lowry, O. H., N. J. Rosebrough, A. L. Farr and R. J. Randall (1951). "Protein measurement with the folin phenol reagent." Journal of Biological Chemistry 193(1): 265-275.

LVWA-SachsenAnhalt. (2017). "Naturschutzgebiete in Sachsen-Anhalt: Selketal." Retrieved 12.09.2017, from https://lvwa.sachsen-anhalt.de/das-lvwa/landwirtschaft-umwelt/naturschutz-landschaftspflege-bildung-fuer-nachhaltige-entwicklung/naturschutzgebiete-in-sachsen-anhalt/selketal/.

Maxwell, K. and G. N. Johnson (2000). "Chlorophyll fluorescence—a practical guide." Journal of Experimental Botany 51(345): 659-668.

McClellan, K. (2006). "Charakterisierung extrazellulärer polymerer Substanzen von Biofilmgemeinschaften unter Einfluss von Photosystem II-Inhibitoren " Diplomarbeit TU Bergakademie Freiberg.

Metzeltin, D., H. Lange-Bertalot, S. Nergui and Y. Li (2009). Diatoms in Mongolia: An as Yet Monospecific Genus from Oligotrophic High Mountain Lakes in the Chinese Province Sichuan, ARG Gantner Verlag KG.

Mulder, C. P. H., D. D. Uliassi and D. F. Doak (2001). "Physical stress and diversity-productivity relationships: The role of positive interactions." Proceedings of the National Academy of Sciences 98(12): 6704-6708.

Natura2000-LSA. (2017). "Bode und Selke im Harzvorland (FFH0172)." Retrieved 12.09.2017, from http://www.natura2000-lsa.de/natura_2000/front_content.php?idart=234&idcat=33&lang=1.

Nikora, V. (2007). 3 Hydrodynamics of gravel-bed rivers: scale issues. Developments in Earth Surface Processes. H. Habersack, H. Piégay and M. Rinaldi, Elsevier. 11: 61-81.

Nõges, P., C. Argillier, Á. Borja, J. M. Garmendia, J. Hanganu, V. Kodeš, F. Pletterbauer, A. Sagouis and S. Birk (2016). "Quantified biotic and abiotic responses to multiple stress in freshwater, marine and ground waters." Science of The Total Environment 540(Supplement C): 43-52.

Passy, S. I. (2007). "Diatom ecological guilds display distinct and predictable behavior along nutrient and disturbance gradients in running waters." Aquatic Botany 86(2): 171-178.

Passy, S. I. (2017). "Framework for community functioning: synthesis of stress gradient and resource partitioning concepts." PeerJ 5: e3885.

Patil, J. S. and A. C. Anil (2005). "Quantification of diatoms in biofilms: Standardisation of methods." Biofouling 21(3-4): 181-188.

Paule, A., V. Roubeix, B. Lauga, R. Duran, F. Delmas, E. Paul and J. L. Rols (2013). "Changes in tolerance to herbicide toxicity throughout development stages of phototrophic biofilms." Aquatic Toxicology 144: 310-321.

Pesce, S., C. Fajon, C. Bardot, F. Bonnemoy, C. Portelli and J. Bohatier (2006). "Effects of the phenylurea herbicide diuron on natural riverine microbial communities in an experimental study." Aquatic Toxicology 78(4): 303-314.

Risse-Buhl, U., C. Anlanger, K. Kalla, T. R. Neu, C. Noss, A. Lorke and M. Weitere (2017). "The role of hydrodynamics in shaping the composition and architecture of epilithic biofilms in fluvial ecosystems." Water Research 127(Supplement C): 211-222.

Rotter, S., R. Gunold, S. Mothes, A. Paschke, W. Brack, R. Altenburger and M. Schmitt-Jansen (2015). "Pollution-Induced Community Tolerance To Diagnose Hazardous Chemicals in Multiple Contaminated Aquatic Systems." Environmental Science & Technology 49(16): 10048-10056.

Roubeix, V., N. Mazzella, L. Schouler, V. Fauvelle, S. Morin, M. Coste, F. Delmas and C. Margoum (2011). "Variations of periphytic diatom sensitivity to the herbicide diuron and relation to species

distribution in a contamination gradient: implications for biomonitoring." J Environ Monit 13(6): 1768-1774.

Schafer, R. B., B. Kuhn, E. Malaj, A. Konig and R. Gergs (2016). "Contribution of organic toxicants to multiple stress in river ecosystems." Freshwater Biology 61(12): 2116-2128.

Schinegger, R., C. Trautwein, A. Melcher and S. Schmutz (2012). "Multiple human pressures and their spatial patterns in European running waters." Water and Environment Journal 26(2): 261-273.

Schreiber, U. (1998). "Chlorophyll fluorescence: new instruments for special applications." Photosynthesis: mechanisms and effects 5: 4253-4258.

Schubert, S. (2015). Schadstoff-induzierte Toleranz autotropher Biofilme gegenüber Schadstoffextrakten der Holtemme. Master of Science, Technische Universität Bergakademie Freiberg & Helmholtz-Centre for Environmetal Research UFZ Leipzig.

Senesi, N. (1992). "Binding mechanisms of pesticides to soil humic substances." Science of The Total Environment 123-124(Supplement C): 63-76.

Shimabukuro, R. H. and H. R. Swanson (1969). "Atrazine metabolism, selectivity, and mode of action." Journal of Agricultural and Food Chemistry 17(2): 199-205.

Smith, W. and T. West (1856). A synopsis of the British Diatomaceæ: with remarks on their structure, functions and distribution; and instructions for collecting and preserving specimens, Smith and Beck, Pub.

Soininen, J. (2004). "Assessing the current related heterogeneity and diversity patterns of benthic diatom communities in a turbid and a clear water river." Aquatic Ecology 38(4): 495-501.

Statzner, B., J. A. Gore and V. H. Resh (1988). "Hydraulic Stream Ecology: Observed Patterns and Potential Applications." Journal of the North American Benthological Society 7(4): 307-360.

Stoodley, P. and Z. Lewandowski (1994). "Liquid flow in biofilm systems." Applied and environmental microbiology 60(8): 2711-2716.

Stoodley, P., K. Sauer, D. G. Davies and J. W. Costerton (2002). "Biofilms as complex differentiated communities." Annual Review of Microbiology 56: 187-209.

Stoodley, P., S. Yang, H. Lappin-Scott and Z. Lewandowski (1997). "Relationship between mass transfer coefficient and liquid flow velocity in heterogenous biofilms using microelectrodes and confocal microscopy." Biotechnology and Bioengineering 56(6): 681-688.

Takahashi, E., J. Ledauphin, D. Goux and F. Orvain (2009). "Optimising extraction of extracellular polymeric substances (EPS) from benthic diatoms: comparison of the efficiency of six EPS extraction methods." Marine and Freshwater Research 60(12): 1201-1210.

Tlili, A., B. Montuelle, A. Berard and A. Bouchez (2011). "Impact of chronic and acute pesticide exposures on periphyton communities." Science of the Total Environment 409(11): 2102-2113.

UCL_Department_of_Geography. (2017). "Diatom Slide Preperation." Retrieved 15.07.2017, from http://www.geog.ucl.ac.uk/resources/laboratory/laboratory-methods/lake-sediment-analysis/diatom-slide-preparation.

Villeneuve, A., B. Montuelle and A. Bouchez (2011). "Effects of flow regime and pesticides on periphytic communities: Evolution and role of biodiversity." Aquatic Toxicology 102(3-4): 123-133.

Wang, C., L. Miao, J. Hou, P. Wang, J. Qian and S. Dai (2014). "The effect of flow velocity on the distribution and composition of extracellular polymeric substances in biofilms and the detachment mechanism of biofilms." Water Science and Technology 69(4): 825-832.

WesternDiatoms. (2017). "Diatoms of the United States." Retrieved 01.08.2017, from http://westerndiatoms.colorado.edu/.

Wicke, D., U. Böckelmann and T. Reemtsma (2008). "Environmental Influences on the Partitioning and Diffusion of Hydrophobic Organic Contaminants in Microbial Biofilms." Environmental Science & Technology 42(6): 1990-1996.

Wu, N., X. Dong, Y. Liu, C. Wang, A. Baattrup-Pedersen and T. Riis (2017). Using river microalgae as indicators for freshwater biomonitoring: Review of published research and future directions.

Yachi, S. and M. Loreau (1999). "Biodiversity and ecosystem productivity in a fluctuating environment: The insurance hypothesis." Proceedings of the National Academy of Sciences 96(4): 1463-1468.

Annex

    I.   Chemicals used for the EPS-assay (see 2.4.6):

Table: Chemicals used for the EPS-assay in chaper 2.4.6. The name of the chemical, their chemical formula (if possible), the producer and the CAS-number are shown.

Chemical	Producer	CAS-Number
3-Hydroxybiphenyl ($C_6H_5C_6H_4OH$)	Sigma-Aldrich	580-51-8
Bovin Serum Albumin (BSA)	BIORAD	not available
Copper(II)-sulfat ($CuSO_4$)	Merck	7758-98-7
D-Glucuronic acid ($C_6H_{10}O_7$)	Sigma	6556-12-3
Folin & Ciocalteu's phenol reagent	Sigma	not available
Humic acid	Roth	1415-93-6
Phenol (C_6H_5OH)	Chemsolute	108-95-2
SDS (Sodiumdodecylsulfat, $NaC_{12}H_{25}SO_4$)	Serva	151-21-3
Sodium hydroxide solution [1M] (NaOH)	Chemsolute	1310-73-2
Sodiumcarbonat, waterfree (Na_2CO_3)	Merck	497-19-8
Sodiumtatrat 2 – hydrat ($C_4H_4Na_2O_6*2H_2O$)	Riedel	6106-24-7
Sodiumtetraborat-Decahydrat ($Na_2B_4O_7*10H_2O$)	Fluka	1303-96-4
Sulfuric acid (95-98%, H_2SO_4)	Sigma-Aldrich	7664-93-9

II.   Solutions compounded and used for the EPS-assay (see 2.4.6):

Table: The solutions and mixtures of solutions with their ratio used for the EPS-assay in chapter 2.4.6 are shown.

Solution	Solvent	Chemical 1 / ratio	Chemical 2
Solution 1	100 mL bi-distilled water	13.4 mL 1M NaOH	0.027 mol Na_2CO_3
Solution 2	10 mL bi-distilled water	$5.64e^{-4}$ mol $CuSO_4$	
Solution 3	20 mL bi-distilled water	0.0023 mol $C_4H_4Na_2O_6*2H_2O$	
Solution 4	Solution 1, 2 & 3	100:1:1 (v:v:v)	
Solution 5	Solution 1 & 3	100:1 (v:v)	
Solution 6	100 mL H2SO4	0.0013 mol $Na_2B_4O_7$	
Solution 7	100 mL bi-distilled water	$1.17e^{-4}$ mol Phenylphenol	1.25 mL 1M NaOh

III.   Timeline of the oxygen and temperature measurements in the flow channel (see 3.2.1)
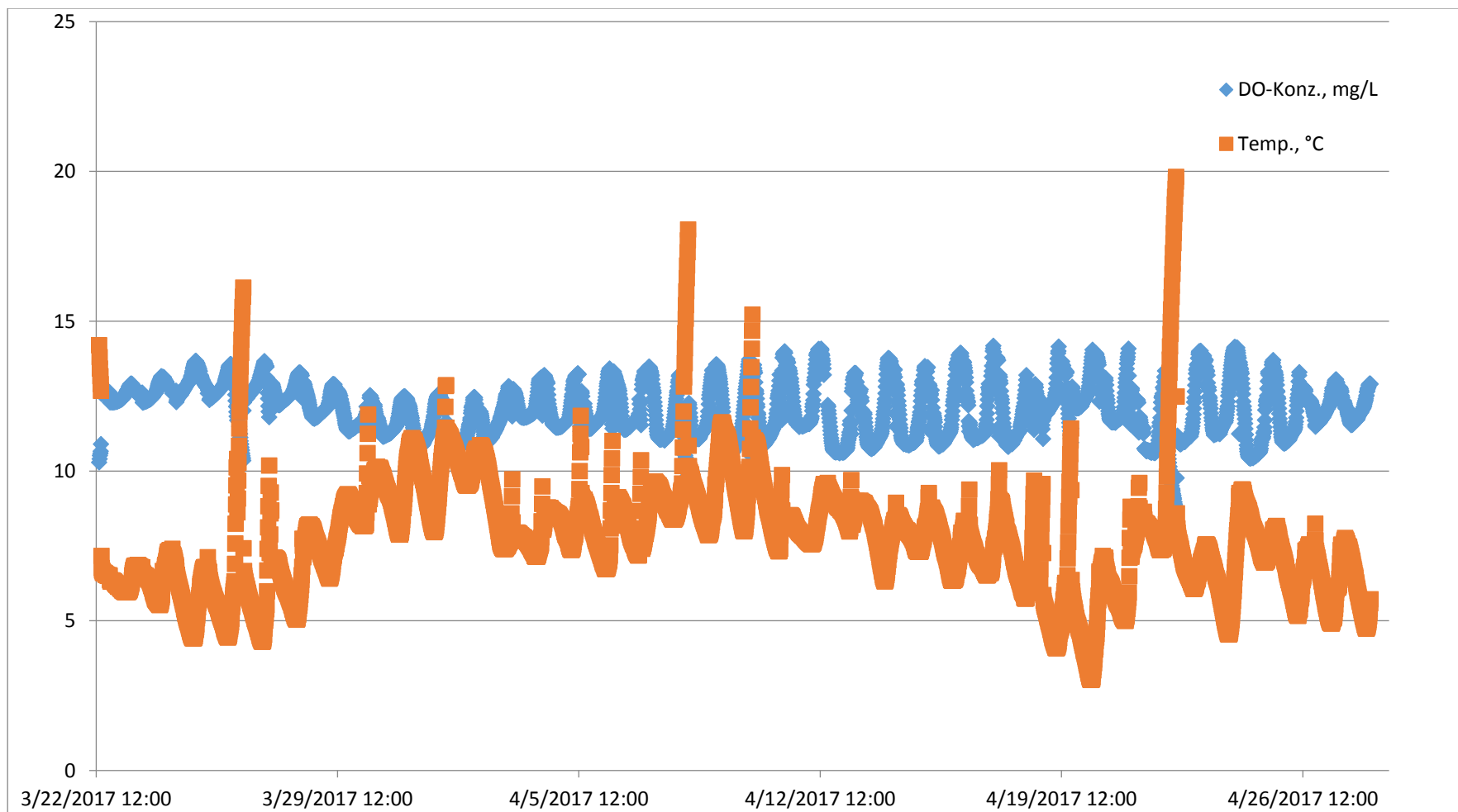
Figure: Course of the oxygen (blue) and temperature (orange) measurements over the whole operation duration of the flume channel.

IV. Media used for the cultivation of *Nitzschia palea* (see 2.5)

Table: Recipe for the diatom media used in chapter 2.5. Chemicals are listed with their concentrations in different units.

Stock solution (dissolve in 1 Liter)				
Chemicals	Concentration			
	g mol^{-1}	g L^{-1l}	mg L^{-1}	mmol L^{-1}
CaCl$_2$*2H$_2$O	147.02	0.919	91.9	0.625
NaHCO$_3$	84.01	0.315	31.5	0.375
NaNO$_3$	105.99	2.126	212.6	2.005
MgSO$_4$*7H$_2$O	177.99	0.925	92.3	0.518
K$_2$HPO$_4$	174.18	0.218	21.8	0.125
Gaffron-TraceElement-Solution (dissolve in 100mL)				
Chemicals	Concentration			
	g mol^{-1}	g 100mL^{-1l}	mg L^{-1}	µmol L^{-1}
H$_3$BO$_3$	61.83	0.3100	3.100	50.135
Na$_2$WO$_4$*2H$_2$O	329.86	0.0033	0.033	0.100
KBr	119.19	0.0119	0.119	0.998
ZnSO$_4$*7H$_2$O	287.57	0.0287	0.287	0.998
Co(NO$_3$)$_2$*6H$_2$O	291.04	0.0146	0.146	0.501
(NH$_4$)NI(SO$_4$)$_2$*6H$_2$O	395.00	0.0198	0.198	0.501
VOSO$_4$	163.00	0.0016	0.0164	0.100
MnSO$_4$*H$_2$O	169.02	0.1690	1.690	11.596
(NH$_4$)$_6$Mo$_7$O$_{24}$*4H$_2$O	1235.86	0.0088	0.088	0.071
KJ	166.01	0.0083	0.083	0.499
Cd(NO$_3$)$_2$*4H$_2$O	308.47	0.0154	0.154	0.499
CuSO$_4$*5H$_2$O	249.68	0.0125	0.125	0.500
Cr(NO$_3$)$_3$*9H$_2$O	400.15	0.0040	0.040	0.099
Al$_2$(SO$_4$)$_3$*16H$_2$O	628.42	0.0366	0.366	0.582

Fe-EDTA-Complex-Solution (dissolve in 100mL)				
Chemicals	Concentration			
	g mol^{-1}	g 100mL^{-1l}	mg L^{-1}	mmol/l
0,1n Solution of FeCl$_3$*6H$_2$O in 0,1m HCl	270.30	2.703	27.030	0.100
0,1n Solution of EDTA	372.30	3.723	37.230	0.100
Fill up each 5 mL to 500 mL with bidistilled water.				
Final mixture	1 L			
Stocksolution.:	20 mL			
Gaffron-TraceElement-solution	0.5 ml			
Fe-EDTA-Complex-Solution.	10 ml			
Silicatsolution.(200 g L^{-1})	1 ml			
Vitamin B$_1$-solution.(1mg 100ml^{-1})	0.5 ml			
Vitamin H-solution.(1mg 100ml^{-1})	0.5 ml			
Vitamin B$_{12}$-solution.(1mg 100ml^{-1})	0.5 ml			
Decoction of soil	20 ml			

V.   Distribution of diatom-guilds after Passy (2007)
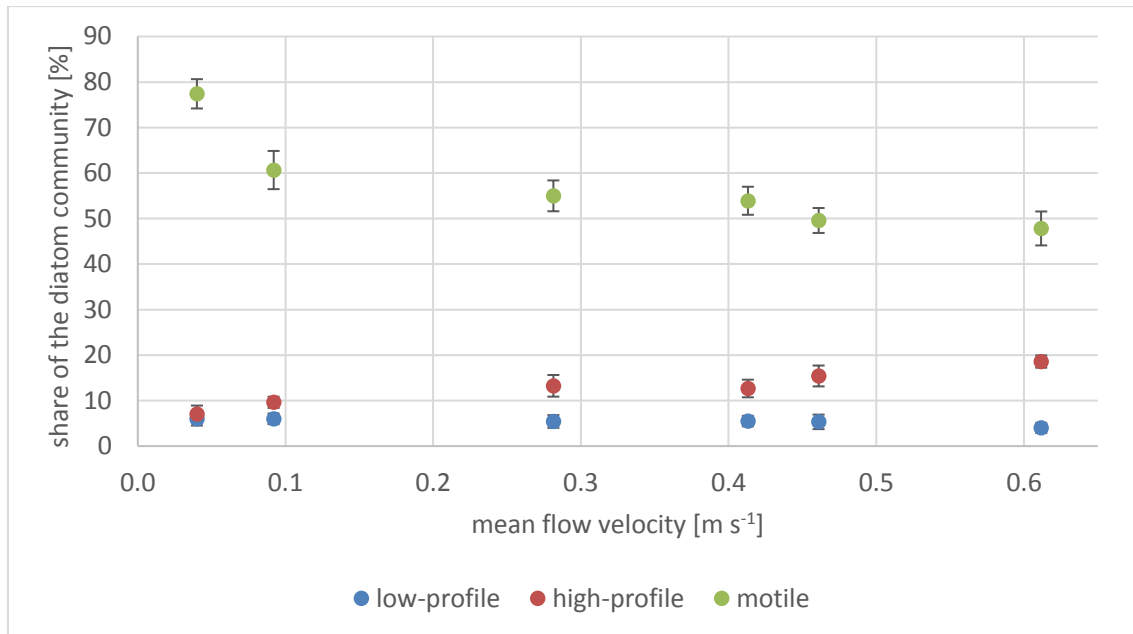
Figure: Based on the morphology-based guild approach by Passy (2007) the diatoms of this study were grouped. Percental distributions (including error bars) are shown at the different mean flow velocities.